The control of selectively exported microRNAs via extracellular vesicles in prostate cancer.

Honours Thesis

Harley Robinson

20th October 2016

Supervisor: Associate Professor Michelle Hill

Co-supervisor: Doctor Alexandre Cristino

<p style="text-align:center">Statement of Authorship</p>

The control of selectively exported microRNAs via extracellular vesicles in prostate cancer.

Harley Robinson

A Research Report submitted for the degree of Bachelor of Biomedical Science (Honours) at

The University of Queensland in October, 2016

School of Biomedical Sciences

Declaration by author:

This research report is composed of my original work, and contains no material previously published or written by another person. However, previously generated RNA-seq data was prepared by Jayde Ruelcke and performed by Nicole Cloonan and previously published mass spectrometry data in Inder *et al.* (2014) was repurposed and reanalysed in this study, with their permission.

I have clearly stated the contribution of others to my research report as a whole, including statistical assistance, survey design, data analysis, significant technical procedures, professional editorial advice, and any other original research work used or reported in my report. The content of my report is the result of work I have carried out since the commencement of my honours research project.

Word Count: 7,687 (Excluding reference list, fig. legends and initial pages as specified p.17 of BIOM6501 honours handbook.)

Lab notebooks (No. TRI-353) and experimental files are stored with the University of Queensland, Diamantina Institute at the Translational Research Institute.

I confirm that my supervisors, Michelle Hill and Alexandre Cristino, have seen a copy of my finished work.

Signature of Author: Date: 19-10-2016

Contents

List of Abbreviations:

BSA	Bovine serum albumin
ddCT	Delta delta cycle threshold
ddPCR	Digital droplet PCR
EDTA	Ethylenediaminetetraacetic acid
ER	Endoplasmic Reticulum
ERp44	Endoplasmic Reticulum protein 44
EV	Extracellular Vesicle
FBS	Foetal bovine serum
FC	Fold Change
FIMO	Find Individual motif occurrences
FUS	Fused in Sarcoma
GFP	Green fluorescent protein
GO	Gene ontology
hnRNP	Heterogeneous Nuclear Ribonucleoprotein
IF	Immunofluorescence
IL-6	Interlukin-6
IP	Immunoprecipitation
ISH	*In Situ* Hybridization
MAPK	mitogen-activated protein kinase
MEME	Multiple expectation-maximization for motif elicitation
miR, miRNA	MicroRNA
MMP-9	Matrix metalloproteinase 9
MVB	Multivesicular bodies
PBS	Phosphate-Buffered Saline
PFA	Paraformaldehyde
PVDF	Polyvinylidene difluoride
RANKL	Receptor activator of nuclear factor kappa-B ligand
RISC	RNA induced silencing complex
RPMI	Rosewell Park Memorial Institute
RT-qPCR	Reverse Transcription quantitative Polymerase Chain Reaction
SEM	Standard error of mean
TAMO	Tools for analysis of motifs
TBS	Tris-Buffered Saline
UTR	Untranslated region
W&B	Washing and binding

Abstract:

Caveolin-1 is a biomarker for aggressive prostate cancer where its overexpression has been linked to metastasis and poor survival. The putative tumour suppressor, cavin-1, was found to neutralize the oncogenic phenotypes induced by caveolin-1 including altered tumour microenvironment. Previous studies from our laboratory suggested that modulating the content of extracellular vesicles (EVs) as a molecular mechanism of cavin-1 tumour suppression. EVs have been proposed to mediate the establishment of the metastatic niche, and cavin-1 was found to reduce the EV levels of known tumour promoting proteins. Interestingly, cavin-1 was also found to reduce the export of oncogenic microRNA miR-148a, without corresponding cellular expression changes. This indicated that export of miR-148a was mediated by a selective export mechanism as opposed to sampling; random uptake of molecules into forming vesicles. Information surrounding this mechanism, such as the proteins involved and the miRNA targets mediated by this mechanism had yet to be investigated.

This project examined the hypothesis where cavin-1 expression in PC3 cells attenuates the EV export of miRNAs, including oncogenic miR-148a, by modulating export of RNA-binding proteins. Differentially exported miRNAs were analysed by an RNA-seq experiment which determined that of the 95miRNAs found in the EVs, 19 were selectively exported. Motif discovery revealed that the majority of the selectively exported miRNAs shared sequence motifs. Mass spectrometry data, Gene Ontology analysis and a motif scanning algorithm identified Heterogeneous Nuclear Ribonucleoprotein K (hnRNPK) as a differentially exported RNA-binding protein that is predicted to bind to an identified selective export sequence motif. hnRNPK changes subcellular localization from multivesicular bodies, which is the originating organelle for exosomes, to endoplasmic reticulum upon the

expression of cavin-1 in PC3 cells. Co-localization experiments were performed using miRNA in situ hybridization and immunofluorescence. These results show that hnRNPK co-localizes with selectively exported miRNA, miR-148a, in cytoplasmic puncta. This co-localization was not observed for PC3-cavin-1 cell lines or with non-selectively exported miRNA, miR-589, in either cell line. Altogether, these results indicate that cavin-1 expression in PC3 cell lines modulate the export of a subset of miRNAs to exosomes by modulating the subcellular localization of miRNA export protein, hnRNPK.

While hnRNPK is commonly detected in cancer derived EVs, this is the first study to reveal a link between EV secreted hnRNPK and miRNA export in cancer. Furthermore, results from this study contribute to the current understanding of miRNA regulation and subcellular localization, extracellular vesicle cargo sorting and prostate cancer aetiology.

Acknowledgements

I wish to extend my appreciation and thanks to my supervisor, Associate Professor Michelle Hill for taking me in as an honours student. Your support and guidance is greatly valued. My co-supervisor, Dr. Alexandre Cristino, also must not go unrecognised for his contributions. Together, they have shaped by understanding of the underlying biology and bioinformatics, but also provided me with valuable experience in the laboratory setting.

Thanks must also be extended to the rest of the Hill lab; Jayde Ruelcke, Anup Shah, Alok Shah, Tam Nguyen, Jeffrey Molendijk, Thomas Stoll, Hui Jiang, Rebecca Lane and Dorothy Loo (proteomics facility manager), for their support and advice throughout. Your feedback and assistance in the lab and during assignment preparation is greatly appreciated.

An additional thank you is given to Jayde Ruelcke and former Hill group member Amanda Oliver. Together you taught me almost all of the wet lab techniques required for the completion of this project.

I am also grateful for the help I received from Dr. Sandrine Roy and Ali Ju for training me on the confocal microscope and with technical support for the fickle microscope.

Thanks to the University of Queensland, the School of Biomedical Sciences and the Diamantine Institute for my acceptance into the honours program and the opportunity to participate in valuable research.

Finally, I wish to thank my family and friends for the support and understanding extended towards me throughout the year. I would not have accomplished this without you.

Introduction:

Advanced Prostate Cancer and Caveolin-1:

Prostate cancer is the second most commonly diagnosed cancer in men (Stewart & Wild 2014). While the primary tumour can be treated and removed efficiently resulting in almost 99% survival, patients inflicted with metastatic prostate cancer possess a reduced 5-year survival rate of 29.3% (SEER 2016). Bone metastasis is the most common complication of advanced prostate cancer which severely impacts survival (Bubendorf *et al.* 2000). This highlights the necessity to identify therapeutic targets and underlying biological phenomena that induce the metastatic phenotype.

Caveolin-1 has been linked to prostate cancer metastasis and has been a speculated biomarker for cancer progression (Gumulec *et al.* 2012; Moon *et al.* 2014; Hayashi *et al.* 2015). This protein binds cholesterol and serves as a structural protein for the formation of caveolae, a specialised lipid microdomain, through interaction with cytoplasmic proteins of the cavin family (Hill *et al.* 2008; Moon et al. 2014). Cavin-1 is required for caveolae formation while cavin-2 and cavin-3 modulate caveolae endocytosis and elongation (Hansen *et al.* 2009; McMahon *et al.* 2009). These proteins are co-expressed and co-localised in healthy human tissue, however in the case of many cancer types only caveolin-1 is expressed (Wu *et al.* 2011; Moumita *et al.* 2015). Increased proliferation, migration and differentiation are a result of the aberrant caveolin-1 expression, yet, the mechanism that links caveolin to these phenotypes is still actively being investigated (Grande-García *et al.* 2007; Chatterjee *et al.* 2015).

Recent studies have shown that cavin-1 is capable of reversing the pro-metastatic action of caveolin-1 in prostate cancer (Moon et al. 2014). Cavin-1 expression inhibited prostate cancer PC3 cell proliferation, migration and anchorage-independent growth *in vitro*, and tumour

growth, metastasis and angiogenesis *in vivo* (Moon *et al.* 2014, Inder *et al.* 2012). Mechanistically, cavin-1 expression altered the tumour microenvironment, including reduction of stromal fibroblasts, secretion of matrix metalloprotein-9 and IL-6 (Aung *et al.* 2011; Moon et al. 2014). The reduced IL-6 secretion was determined to be through extracellular vesicle (EV) release (Inder *et al.* 2014). Intriguingly, cavin-1 expression also attenuated the EV-mediated release of microRNA-148a, which was previously reported to mediate bone metastasis through osteoclastogenesis (Cheng *et al.* 2013; Inder et al. 2014). These results suggest that one mechanism of cavin-1 tumour suppression in prostate cancer occurs partly by modulating EV microRNA content.

Horizontal Transfer of MicroRNAs via Extracellular Vesicles:

Secreted membrane-bound vesicles, called extracellular vesicles, are important mediators of intercellular communication (Pegtel *et al.* 2014). EVs are comprised of vesicles predominately from two different sources, exosomes and microvesicles (Fig.1). Exosomes are defined as 40-100nm diameter extracellular vesicles which are released upon fusion of the multivesicular bodies with the plasma membrane (Gu *et al.* 2014). Whilst similar in function and biochemical markers, microvesicles (≥100nm) differ from exosomes by being released from budding of the plasma membrane (Minciacchi *et al.* 2015). This report focused on a mixed population of EVs as past research also utilized mixed populations when analysing EV content. EV cargo consists of cytoplasmic material, functional RNA and proteins where uptake of this content had been reported to influence a range of biological processes, such as the selective export of cytokines in immunological responses, mediating homeostasis and stress response (McKechnie *et al.* 2006; Wysoczynski and Ratajczak 2009; Hedlund *et al.* 2011). Recent studies have reported that cancer-derived EVs absorbed into recipient cells are able to induce the establishment of the pre-metastatic niche in cancer progression and tumour microenvironment modifications (Costa-Silva *et al.* 2015; Ramteke *et al.* 2015). Primarily
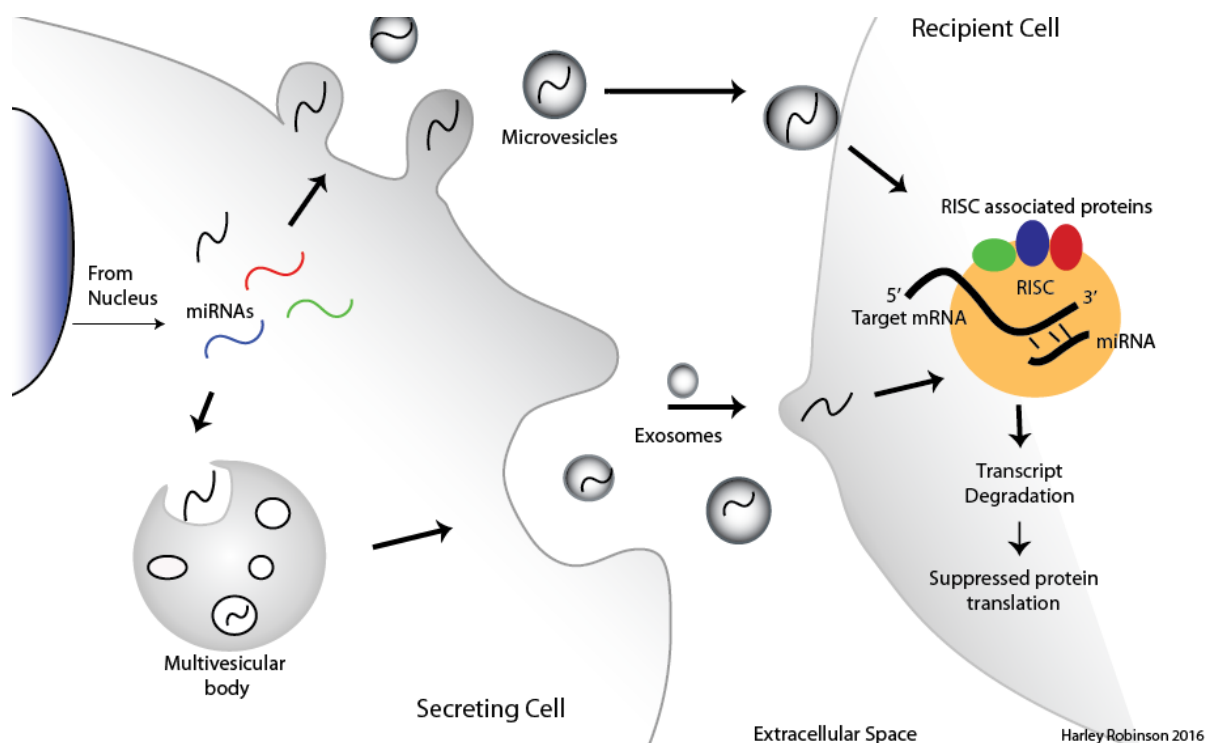
Figure 1: *Diagrammatic representation of microRNA extracellular vesicle transport.* EVs are formed in two different ways: from budding of the plasma membrane to form microvesicles and from fusion of the multivesicular bodies (MVBs) with the plasma membrane to release exosomes. EV contents includes miRNAs. These miRNAs bind to its target mRNA by complementary base pairing and recruit the RISC complex and associated proteins when absorbed into the recipient cell. This enables down regulation of proteins in the recipient cell by degradation of the transcript. (Illustration completed on Adobe Illustrator CC 2014)

this has been attributed to the proteomic EV content being transferred to the target cell, such as introduction of beta-catenin, epidermal growth factor receptor and major elements of the MAPK pathway (Dovrat *et al.* 2014; Kharmate *et al.* 2016; Song *et al.* 2016). Yet, more intriguing is the discovery that exported microRNAs may be associated with this function.

MicroRNAs (miRNAs, miRs) are small non-coding RNAs found to be involved in most developmental and pathological processes due to its ubiquitous gene regulatory function. The functional miRNA sequences (~19-24 nt) are derived from longer transcripts that undergo processing and shuttling events to give rise to functional mature sequences, known to induce RNA degradation (Ha and Kim 2014). Typically, the mature miRNA sequence interact with the 3' untranslated region (3'-UTR) of its target transcripts and guides the multi-protein RNA induced silencing complex (RISC) to destine these molecules for degradation or translational inhibition (Djuranovic *et al.* 2012) (Fig. 1). A 2009 estimate predicted that approximately 60% of the mammalian genome is able to be directly mediated by the miRNA RISC mechanism where a single miRNA can target hundreds of transcripts (Friedman *et al.* 2009). This indicates the necessity of tight temporal and spatial control over miRNAs to prevent dysregulation of vital pathways. MicroRNAs in the extracellular space was expected to be controlled by the high content of RNases in the extracellular space (Reddi and Holland 1976; Tsui *et al.* 2002). However, recent studies show that EV-contained miRNAs are protected from this degradation and are absorbed into recipient cells, thus evoking their canonical function in a potentially diverse cell type (Kosaka *et al.* 2010; Montecalvo *et al.* 2012) (Fig.1).

Secreted MicroRNAs in Prostate Cancer:

Earlier work from our lab utilizes the caveolin-1/cavin-1 system to investigate the role of caveolin-1 in prostate cancer (Inder *et al.* 2014). Interestingly, the addition of cavin-1 to PC3 cells modified extracellular vesicle (EV) content, a pathway unrelated to the canonical

function of caveolin or cavin-1. In addition to limiting adhesion independent growth, hyper-proliferation and EV protein content of PC3 cells, the ectopic expression of putative tumour suppressor, cavin-1, modified miRNAs found within EVs; specifically miR-148a (Inder et al. 2014). Expression of miR-148a in bone marrow was reported to induce osteoclastogenesis by targeting an inhibitory transcription factor, MAFB, of the RANKL-induced osteoclastogenesis pathway, where the inverse was observed upon miR-148a inhibition (Cheng *et al.* 2013). Bone fracture, pain and fragility are common co-morbidities associated with the bone metastasis-mediated prostate cancer due to increased bone resorption (Luz and Aprikian 2010). Therefore the export of miR-148a from pro-metastatic prostate cancer cell line is consistent with clinical findings and may be a regulator of metastatic progression. Interestingly, the expression of cavin-1 does not modify the cellular level of miR-148a, only the EV content (Inder et al 2014). This suggests that cavin-1 regulates the miRNA sorting to EVs and therefore export. Selective export of miRNAs in EVs had been observed in other studies, some of which links these miRNAs with disease states, particularly cancer metastasis (Palma *et al.* 2012; Zhou *et al.* 2014). Yet, the mechanism that governs this selectively is mostly unknown.

A recent clue was provided by Villarroya-Beltri *et at*. (2013), who reported that sumoylated ribonucleoprotein, hnRNPA2B1 mediate the export and subcellular localization of particular miRNAs in T-lymphocytes. Typically, the hnRNP family are involved in mRNA processing within the nucleus for translational control, mRNA stability and subcellular localisation. Yet, this is the first reported case of EV/multivesicular body localisation occurring from this mechanism and one of the first reports of its ability to bind to miRNAs (Mili *et al.* 2001; Dreyfuss *et al.* 2002). Further questions arise due to this finding, such as the use of other hnRNP proteins for miRNA subcellular localization, how hnRNPs are targeted to the EVs and whether this protein family could be responsible for miRNA EV export in other cell types and stimuli.

Hypothesis and Aims:

Based on the above, we hypothesised that cavin-1 expression in PC3 cells attenuates the EV export of oncogenic miR-148a by modulating export of RNA-binding proteins (Fig.2), similar to the mechanism identified by Villarroya-Beltri *et al.* (2013). Given that RNA-binding proteins select for targets by binding conserved RNA sequences, known as motifs, we further hypothesize that miR-148a and other RNA targets will share a motif that enable their selective export over other microRNAs. The following aims were devised to address these hypotheses:

1. Assess the EV microRNA species that are modulated by cavin-1 expression in PC3 cells.

2. Identify candidate export protein(s) that participate in microRNA EV export.

3. Verify the interaction between candidate protein and microRNA by *in situ* and *ex vivo* experimental methods.
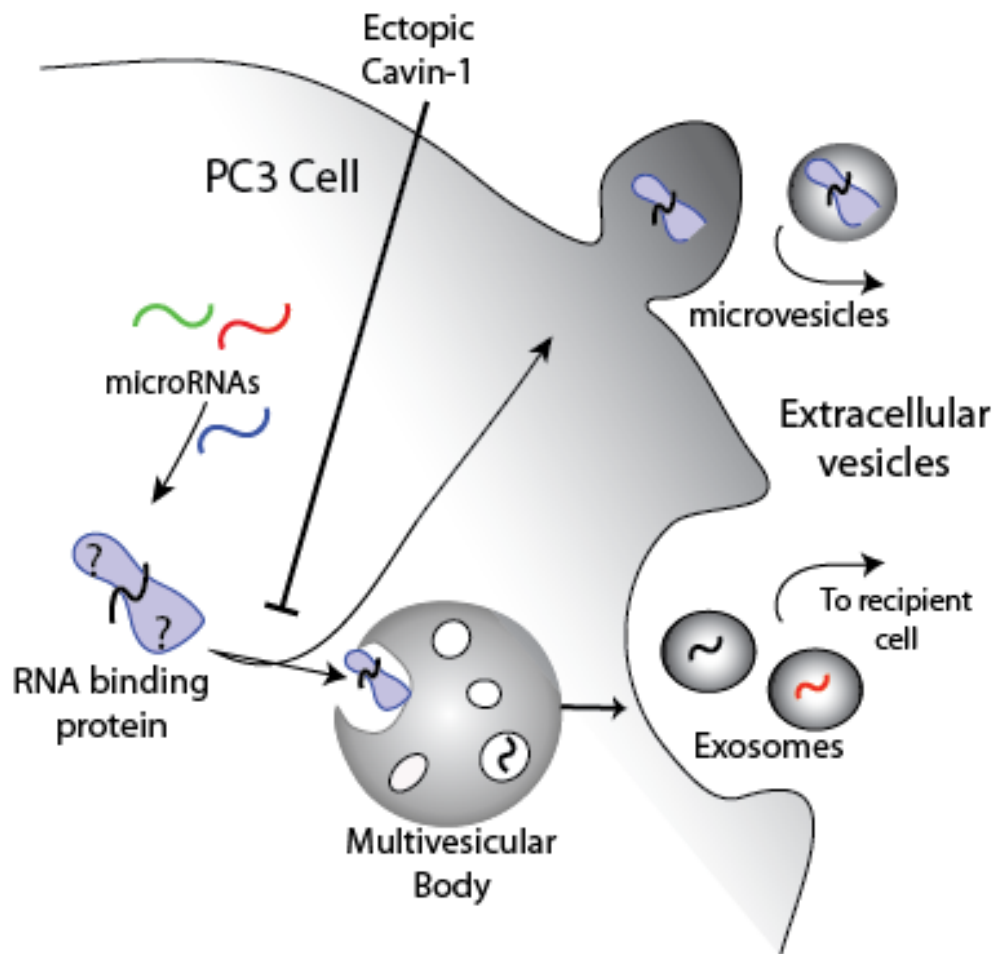
Figure 2: *Diagrammatic representation of the proposed miRNA export mechanism mediated by cavin-1 expression in PC3 cells.* It is hypothesised that RNA-binding proteins involved with the miRNA export mechanism are exported in the PC3-derived EVs. However, ectopic expression of cavin-1 to these cells will reduce the export of RNA-binding proteins and therefore miRNA export.

Methods and Materials:

Reagents:

Trypsin-EDTA (Gibco), Roswell Park Memorial Institute (RPMI) 1640 media (Sigma), Fetal Bovine Serum (FBS) (Bovogen), Phosphate Buffered Saline (PBS) (Amresco Inc), Geneticin G418 Antibiotic (Invitrogen). Antibodies used: rabbit anti-hnRNP K (CST), mouse anti-hnRNPK (Abcam), rabbit anti-CD9 (CST), rabbit anti-ERp44 (CST), normal rabbit IgG (CST), anti-mouse AlexaFluor568 and anti-rabbit AlexaFluor674 (ThermoFisher). All antibody dilutions used were per the manufactures' suggestion.

Cell culture:

Previously generated PC3 cell lines containing GFP or GFP tagged cavin-1 (referred to as PC3-cavin-1) were cultured in 5% FBS/RPMI1640 media in a 5% CO_2 incubator set to 37°C. Ectopic gene expression levels were confirmed by immunoblotting for GFP (not shown). G418 antibiotic drug (0.1 mg/ml) was added to these cultured cells to select for GFP expressing cells.

Differential miRNA expression:

The results from a previously conducted RNA-seq experiment, prepared by Jayde Ruelcke (Hill lab) and conducted by Nicole Cloonan (QIMR), were utilized for this analysis. Briefly, small RNAs were collected from EVs derived from PC3-GFP and PC3-cavin-1 cell lines and the cognate cells, resulting in 3 biological replicates. These RNAs were multiplexed, sequenced via Illumina sequencing, aligned and assessed for raw counts for miRNAs in cell and EVs (completed by Nicole). Analysis was performed using these raw counts. An R package, DESeq2, had normalized these counts to fit a negative binomial distribution and excluded microRNA data that possessed low to no counts (≤10 counts) for miRNA species across the triplicates and conditions (GFP and cavin-1), allowing for only relevant microRNAs to be assessed. Applying the function makes comparisons of expression or content between GFP and cavin-1 cell conditions and returns this in the form of log2 fold

change (FC), Wald test p-value and a false discovery rate corrected p-value. This analysis was completed separately for cell and EV miRNA content. By using the log2FC values for each miRNA, comparisons were made between cell and EV expression by taking the difference in the form of $FC_{EV}-FC_{cell}$. Frequency disruption graphs were plotted by measuring the frequency of FC-FC in increments of 0.05. GraphPad Prism was used to generate this graph and line of best fit added by analysis of 'Sum of two Gaussians'.

Extracellular Vesicle Extraction and RNA extraction:

Cells were grown to 70% confluency prior to the addition of fresh serum free RPMI1640 media on 15cm Petri dishes. The conditioned media was collected after 24hrs of incubation and concentrated in a 10kDa ultracentrifugation filter tube (Sigma) until 1mL of concentrated media was achieved. Concentrated media was processed through an exoRNeasy midi kit (Qiagen) to extract the total EV RNA as per manufacturer's instruction. A sample of the cognate cells were also collected for comparison. The total cellular RNA was collected using the MiRvana kit as per manufactures' instruction (Invitrogen). Nanodrop was used to assess to the purity and concentration of the RNA, where samples with an $A_{260/280}$ approximating 1.8 were be used for further experimentation.

Reverse Transcription quantitative Polymerase Chain Reaction (RT-qPCR) and preparation:

Poly-adenylation was completed using the E.coli polyadenylation enzyme and associated buffers (NEB) using a standard protocol (Balcells *et al.* 2011). This was immediately followed by cDNA conversion using the Superscript II Reverse Transcriptase and 0.1µg/µL oligo DT (Invitrogen) as per standard Invitrogen protocol. RT-qPCR was performed on the samples with primers specific to miR-363-3p, 148a-3p, 10b-5p, 200a-3p, 30a-3p and 574-5p (IDT). Mir-125a-3p was used as the reference gene due to producing the same level of expression in EVs derived from both GFP and cavin-1 PC3 cells based on the RNA-seq data. Delta delta CT statistics were completed by comparing between GFP and cavin-1 cell lines

for the target and reference genes. Bar graphs generated by GraphPad Prism 6 and statistics calculated using a non-parametric two-sided T-test (Mann-Whitney U-test).

Motif Discovery and Assessment:

TAMO (Tools for Analysis of MOtifs) Unix package was used to determine shared RNA-motifs within the differentially exported miRNA data set. The MEME algorithm was used to find a motif 4 to 10 nucleotides in length mapped amongst the inputted miRNA sequences with at least 70% conservation. The resulting motif was compared to the sequences of all expressed miRNAs in the PC3 cells to determine specificity to the differentially exported miRNAs using the sitemap algorithm using default parameters. Comparing motifs to the binding sequence of hnRNPK to determine matches was performed using FIMO algorithm with default parameters. All algorithms generate statistical analysis in the form of a p-value. Sequence logos were generated using WebLogo online logo generator.

Proteomic Analysis:

Previously published proteomics data were retrieved from an online supplementary data file (Inder *et al.* 2012). The RNA binding annotation for the significantly altered proteins, listed in the supplementary data file, were analyzed using the biomaRt R package for Gene Ontology (GO) annotation (GO:0003723). Venn diagram was generated using an online graphing and diagram tool, Draw.IO.

Co-localization by Immunofluorescence Confocal Microscopy:

Cells were grown to 70% confluency on coverslips prior to fixation with 4% PFA for 30 minutes at room temperature. All further incubations were performed at room temperature. After washing with PBS, 0.1% Triton-X100 in blocking solution (1% BSA/PBS) was added to the coverslips to block and permeabilize the cells. After 30 minutes of incubation, the coverslips were washed and primary antibodies in blocking solution were then incubated with the coverslips for 1 hour at room temperature. Coverslips were then washed 3 times with PBS

prior to incubation with secondary antibodies in blocking buffer for 1 hour in the dark at room temperature. After washing 3 times in PBS, 1:1000 dilution of DAPI in blocking solution was incubated with coverslips for 10 minutes in the dark, followed by additional PBS and MilliQ water washing. Excess water was removed by Kimwipe prior to mounting on slides with 8μL Prolong Diamond (Invitrogen). Slides were dried for 24 hours at 37°C prior to imaging with the Olympus Confocal microscope. Pseudocolour and scale bar was added by the FluorView software for the Olympus microscope.

MicroRNA *In situ* Hybridization:

Cells were grown to 70% confluency on coverslips prior to fixation with cold 100% methanol. Coverslips were then washed thrice with PBS and incubated in the dark overnight at room temperature in 50 pmole of Cy5 conjugated antimiR in oligo hybridization buffer; 50mM NaCl, 1mM Tris-Cl (pH 8.0), 0.1mM EDTA (pH 8). Cy5-scrambled-miR-148a oligo (5'-Cy5-GAUUCAUAGCGAUCCUUACAUG-3') was used as a negative control and anti-miR-589 was used as a biological control as this miRNA should not bind or co-localize with hnRNPK. Excess antimiR was removed by washing thrice in PBS before 4% PFA fixation for 30minutes. Subsequent steps were performed as per immunofluorescence protocol for hnRNPK localisation with Alexa Fluor 568 secondary antibody. Spectral bleed through of Cy5 and Alexa Fluor was checked prior to data collection by individually staining a sample with antibody or hybridizing Cy5-antimiR and visualizing neighbouring channels (data not shown).

Immunoprecipitation:

Protein G DynaBeads were washed thrice in washing and antibody binding (W&B) buffer to remove storage reagents using the DynaMag2 magnet to separate and fix beads. W&B contains 0.1M Sodium Acetate and 0.05% Tween-20 diluted in distilled water. 1μL of rabbit anti-hnRNPK were added to 200uL of W&B buffer, added to the beads and incubated on a

rotating wheel for 40 minutes. 1μL of normal rabbit IgG were also prepared separately as a negative control. Excess antibody were removed by washing with W&B buffer thrice.

Cellular components were cross-linked by adding 1% formaldehyde/PBS for 8 minutes at room temperature. After washing with room temperature PBS, cells were scraped into tubes. Cell pellets were lysed by 20 minute incubation, on ice, with modified lysis buffer; 1% Triton-X, 20mM Tris (pH7.5), 150mM NaCl, 1x Protein Inhibitors (1mg/ml of Aprotinin, Antipain, Pepstain A, Leupetin and 500mM Benzamidine), 0.5mM MAEBSF, 0.5mM Na$_3$VO$_4$, 10mM NaF and 0.1mM sodium pyrophosphate. After incubation, lysates were centrifuged at 14,000g, for 5 minutes at 4°C and supernatant transferred to a new tube. Cell lysate were diluted 1:5 in lysis buffer and added to antibody-bead tube. This was incubated for 45minutes at 4°C on a rotating wheel prior to washing 5 times with lysis buffer. Protein-RNA crosslinked sample were eluted by incubation with SDS-PAGE buffer for 5 minutes at 95°C. This were then analyzed with western blot for protein level, or TRIzol extraction for RNA level. TRIzol (500μL) was added to the beads and incubated at 95°C for 5 minutes to reverse the crosslink. Subsequent steps were performed as per standard TRIzol extraction protocol (Lee *et al.* 2011). Quantification of RNA was performed by Nanodrop analysis.

Western blotting:

Sample buffer were added to whole cell lysate or EV lysate sample to reach a final 1X concentration and protein denatured by incubation at 95° C for 5minutes if denaturation was not already performed. BioRad Precession Plus protein ladder were loaded into a 12.5% SDS-PAGE gel with 4% stacking gel. Blanks (10uL of SDS-PAGE buffer) were placed in wells either side of the ladder. Samples were added in equal amounts to the wells. SDS-PAGE buffer were added to any unfilled wells to maintain consistent salt concentrations across the gel. Gels were ran at 80V until sample stacked, then increased to 100V until the dye front reached the end of the gel. Wet transfer was completed following a standard

procedure and reagents to transfer protein to a fluorescent PVDF membrane (Towbin *et al.* 1979). Membrane was subsequently blocked in 3% BSA/PBS with 0.1% Triton-X for 30minutes to prevent non-specific antibody binding. hnRNPK antibody was diluted 1:1000 in blocking buffer in a 50mL falcon tube. Membrane was added face up into the tube, avoiding air bubbles and incubated for 1.5hrs at room temperature on a roller. This was followed by washing thrice in TBS-Tween-20 (0.1%). IRdye800W anti-mouse (Li-Cor) was added to blocking solution to a final concentration of 1:7,500, kept in the dark and incubated with the membrane for 1hr. After subsequent washing thrice with TBS-tween, membrane was washed again with PBS and dried in the dark. Odyssey (Li-Cor) imaging system visualized the bands in two channels (700 and 800nm) with the ImageStudio software.

Results:

MicroRNAs are selectively exported from prostate cancer cells.

MicroRNA-148a was previously found to be selectively exported from the PC3 cell line where this export was truncated by ectopic expression of cavin-1 (Inder et al. 2014). However, this analysis had not considered other miRNAs that may also be regulated by cavin-1. To determine all PC3-EV miRNAs that are modified by cavin-1 expression, our lab conducted a comprehensive RNA-seq analysis to quantify the miRNAs in EVs and cognate cells. From 3 biological replicates, a total of 95 miRNAs were detected in EVs from PC3 cell lines. Comparison between GFP and cavin-1 cell lines through differential expression analysis (DESeq2) revealed a total of 12 significantly (p ≤ 0.05) modified miRNAs in the EVs (fig. 3a), including miR-148a. The previous study revealed that reduction of EV-contained miR-148a was not simply due to a reduction of its cellular expression level. Here, I wanted to determine if this trend persists with additional miRNAs. Comparison between cellular and EV modifications induced by cavin-1 reveals a subset of 5 miRs that are dramatically reduced in the EVs with little change in total cellular expression. These are the miRNAs likely to be acted upon by the proposed protein mediated export, attenuated by cavin-1 expression. In contrast, 6 of these miRNAs (miR-19a-3p, 10b-5p, 146a-5p, 363-3p, 149-5p and 222-3p) present with proportionate cellular expression change that could explain the decrease or increase in EV miRNA content. This process is known as sampling, where miRNAs in the cytoplasm are taken into the forming EVs due to proximity as opposed to protein mediated export that would confer some selectivity. These results suggest that both sampling and selective export of miRNAs can occur in PC3 EVs.

A subset of significantly modified miRNAs across the sampling and selective export groups were selected for RT-qPCR validation; Selective export reduced by cavin-1; miR-30a-5p, miR-148a-3p, miR-200a-3p, miR-10b-5p, selective export induced by cavin-1; miR-574-5p
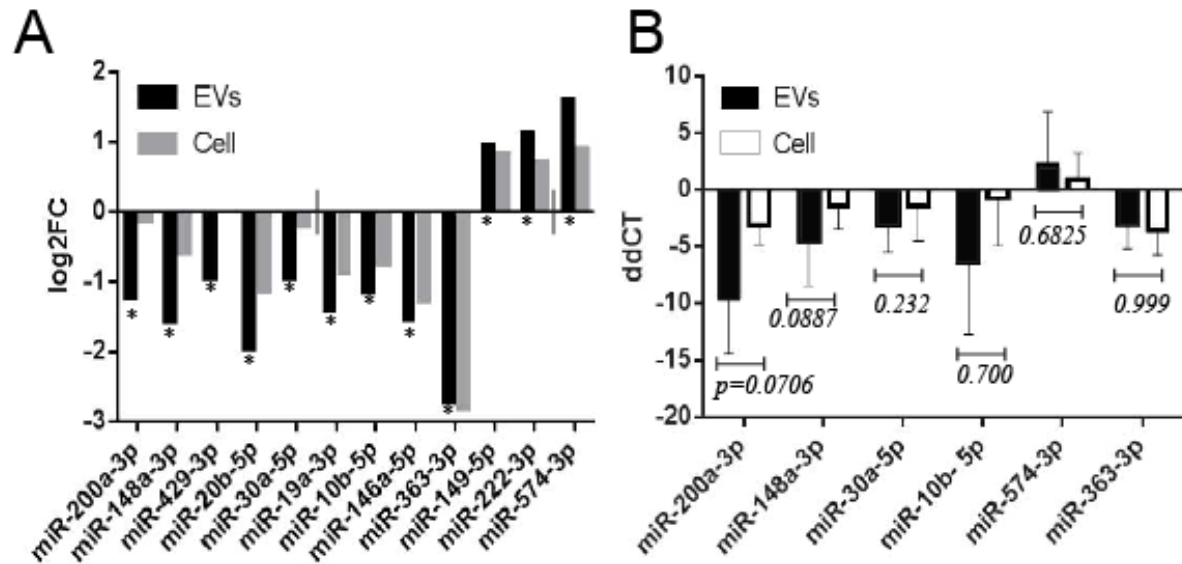
Figure 3: *Expression ofcavin-1 in PC3 cells modifies EV microRNA levels.* **A**) RNA-seq was performed previously on microRNAs extracted from the EV and cellular content of PC3-GFP and PC3-cavin-1 cells. DESeq2 analysis compared PC3-GFP to PC3-cavin-1 EV content (black), expressed as log2FC, to determine the effect of cavin-1 on EV miR level. miRs that were significantly modified (* $p \leq 0.05$, by Wald test) in the EVs were plotted. Analysis was repeated on cellular content (grey) for each of the miRs significantly modified in the EVs. This reveals that cavin-1 has an effect of miR EVs where some effected miRs are not modified in the cell. **B**) RT-qPCR was performed to validate the RNA-seq data. This was performed on EV and cellular RNA content extracted from GFP and cavin-1 PC3 cells to determine relative amount of miR-200a-3p, 148a-3p, 30a-5p, 10b-5p, 574-3p and 363-3p (n > 3). The samples were independent of the RNAseq samples. Delta-delta CT (ddCT) was calculated and plotted (ddCT + SEM error bar) by comparing expression of targets to miR-125a-3p. This miR was unchanged in the EV and cell by cavin-1 expression. A Mann-Whitney U test compared EV change to the cellular change for each of the miRs. This analysis confirms the trends found from the RNA-seq data.

and sampling; miR-363-3p. Independent biological replicates of EV and cellular small RNAs were prepared and used for RT-qPCR. As shown in Figure 3B, the trend first displayed by the RNA-seq data (Fig. 3a) is maintained. Consistent with the RNA-seq data, cavin-1 expression led to higher magnitude of reduction of miR-30a-5p, 148a-3p, 10b-5p and 200a-3p in EVs compared to the reduction of their cellular levels. Inversely, miR-574-3p was increased due to the presence of cavin-1 in the EVs, and miR-363-3p is confirmed to be not selectively exported by cavin-1. This result establishes that some miRNAs are indeed selectively exported from PC3 cells, where cavin-1 modulated this export.

Distinct sequence motifs are overrepresented in differentially exported microRNAs.

Protein-RNA interactions are dictated by specific nucleic acid sequences, or motifs, that are conserved across the targeted RNAs. Here, we attempted to assess whether the selectively exported miRNAs share a sequence motif to explain their selective export. Based on the initial statistical analysis, only 5 miRNAs were selectively exported (fig.3a). However, motif discovery with only 5 miRNAs was not adequate to establish a significant motif (data not shown), so additional miRNAs were selected for this analysis based on their relative levels of change between EV and cell. All 95 miRNAs recorded in the EVs from the RNA-seq data were compared to their cellular change in the form of $\log_2FC_{EV}$- $\log_2FC_{cell}$ (Fig.4a). This provides a single value that reflects how different the EV modifications are from the cell, where selective export results in a large negative (cavin-1 reduces export) or positive (cavin-1 enhances export) value and sampling approximates 0. Expressing these values as a frequency distribution plot reveals how prevalent each form of export is (Fig.4b). This yielded a large population of miRNAs that undergo sampling, around 0.1, but also a small peak at -0.45. The miRNAs that were validated in RT-qPCR were noted on the graph to demonstrate where they fit into this distribution. This shows the selectively exported 200a-3p, 148a-3p and 30a-5p to the far left of the graph, with 363-3p in the sampling population (FC-FC≈0.1) and 574-3p to
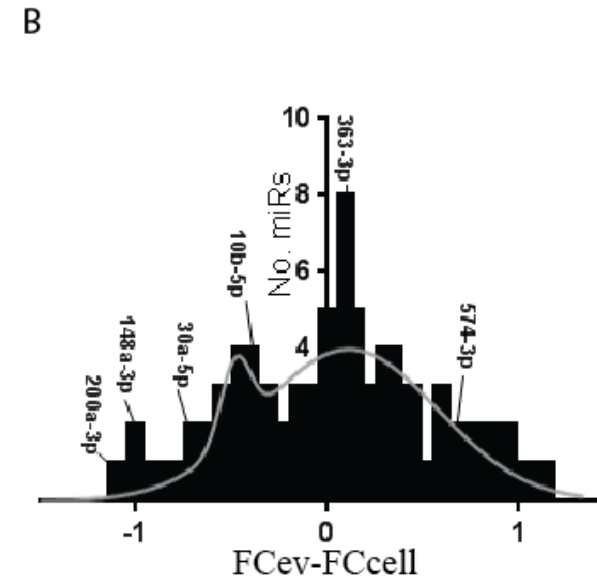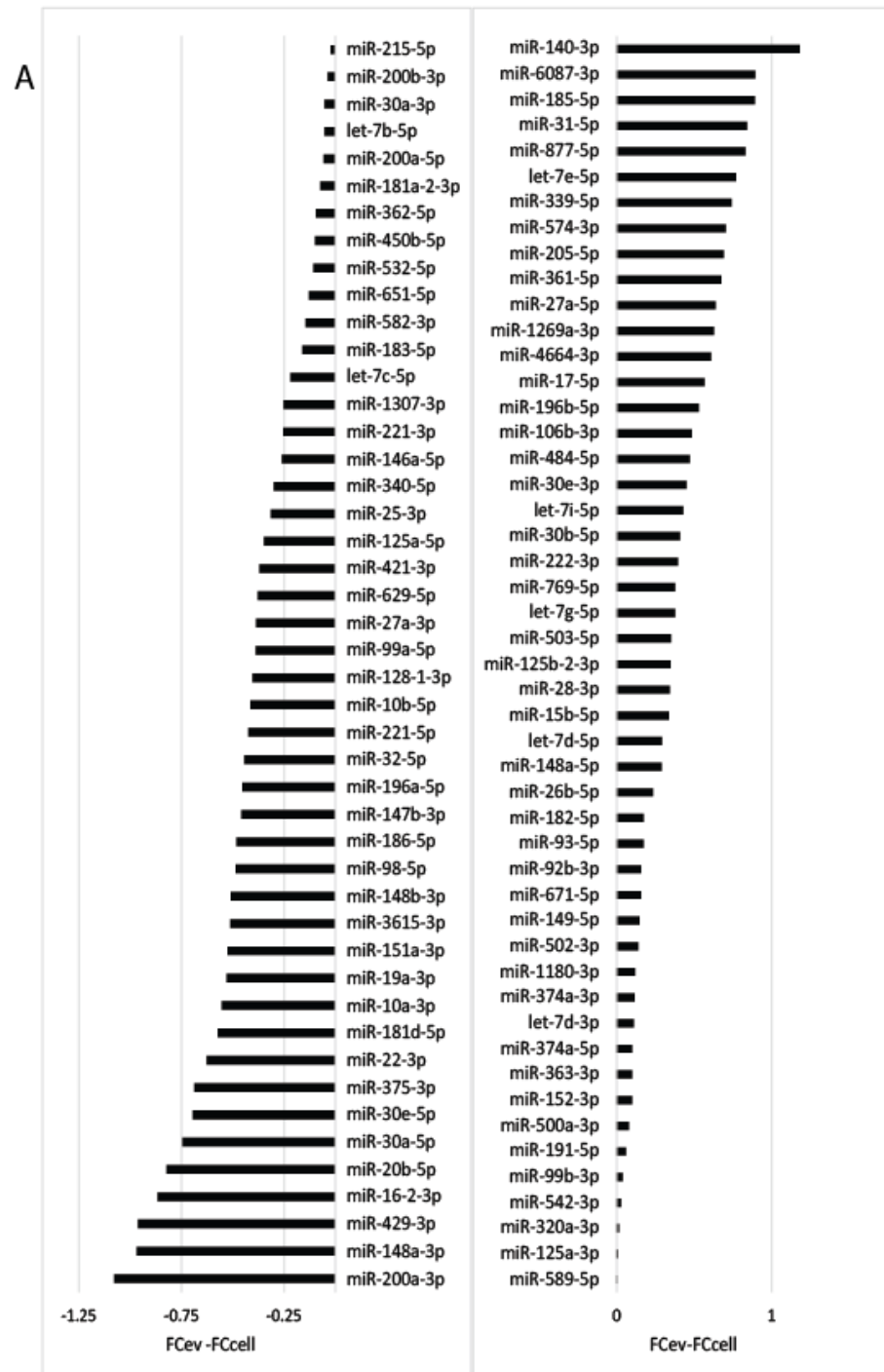
Figure 4. *Comparison of microRNA EV and cellular changes inflicted by cavin-1 expression.* **A**) All 95 miRs detected in the EVs were analysed to determine selective or sampling mediated export. Bar graph displays the difference between FCev and FCcell for each miR. **B**) Frequency distribution graph of the FC-FC value, by increments of 0.05, and experimentally validated microRNAs. Line of best fit modelled by sum of two Gaussians. Two major populations are present: sampling peak at 0.1 and selective export at -0.45.
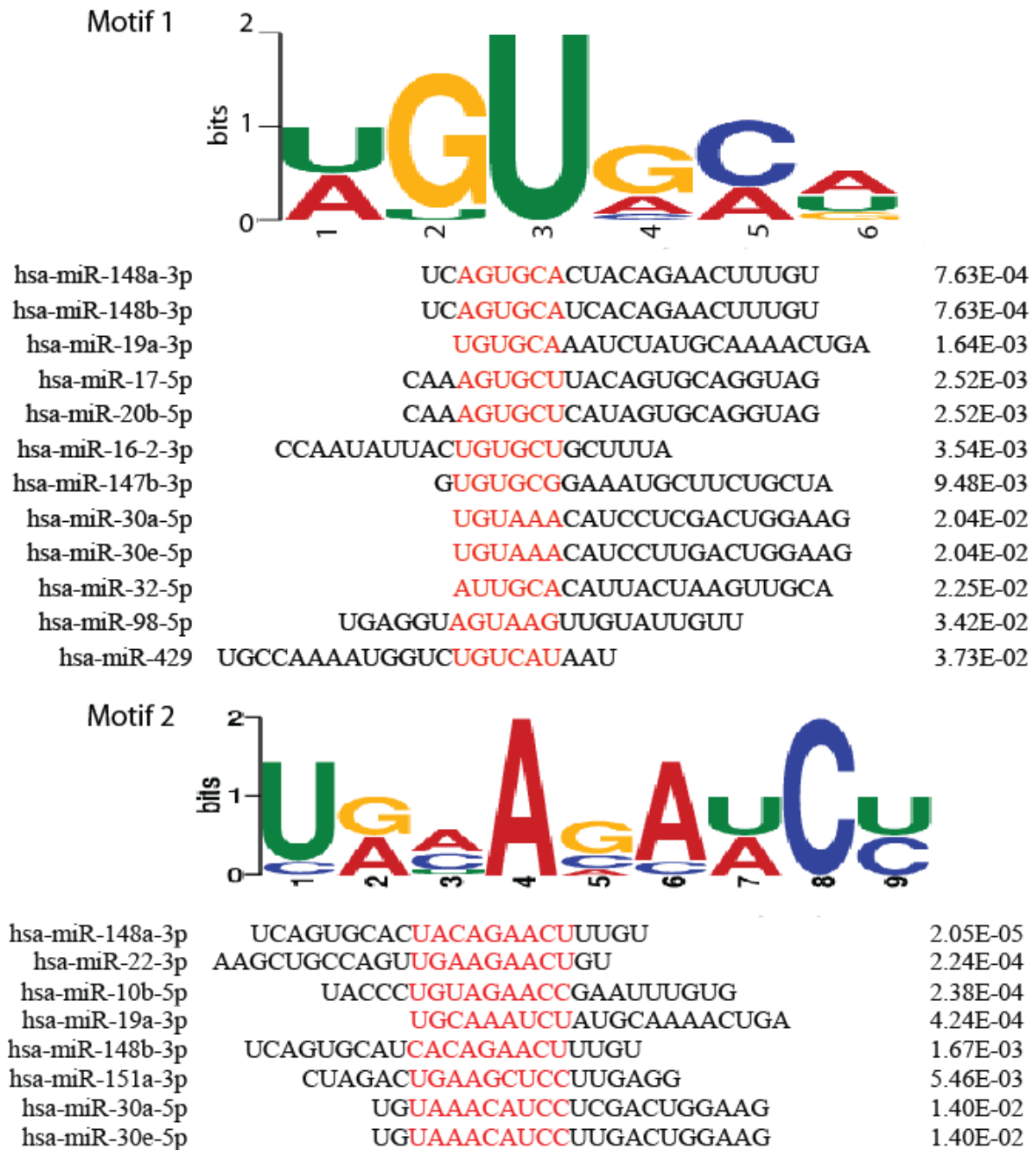
the right of the graph. This corresponds to the groupings established previously (Fig.3a).

Hereby, miRNAs that correspond to a FC-FC of -0.45 or lower are considered selectively

exported for this motif discovery. 19 miRNAs fulfill this criteria.

Motif discovery, using the MEME algorithm, was used to define stretches of RNA that are

shared amongst the differentially exported miRNAs which would be targeted by the miRNA

export protein. This analysis returned two distinct motifs that are enriched in the miRNA

group that possess reduced export upon cavin-1 expression (Fig.5). These motifs are present

within 14 of the 19 miRNAs within this group. Individually, the first motif matches to 12 of

the 19 miRNAs and the second correlated to 8 of the 19. As the miRNAs found in the

sampling group should not bind to the export protein, it is likely that sampled miRNAs would

not contain these motifs. Using the sitemap algorithm on all of the 95 miRNAs determines all

matches of the motif to the EV contained miRNAs, including both selectively exported and

sampled miRNAs. This returned no significant matches between the motifs and the sampled

miRNAs. This reveals potential binding sites the export protein may be able to bind to evoke

specificity and selectivity of the targets.

Candidate proteins are present in EVs with RNA binding ability.

To identify candidate proteins that could mediate this selective miRNA export, EV protein

content was assessed for (1) differential export upon cavin-1 expression and (2) RNA-binding

ability. The analysis used a previously published quantitative proteomic dataset (Inder et al.

2012). A total of 120 EV proteins were differentially exported upon cavin-1 expression

(Fig.6). Since miRNAs of interest were down-regulated by cavin-1, the 109 down-regulated

proteins were selected for further GO analysis to determine whether these proteins had

previously reported RNA-binding capacities. Together, this yields a total of 5 differentially

exported RNA-binding proteins: FUS, hnRNPK, snRPD3, HSP90B1 and ILF2. As members

Motif 1

miRNA	Sequence	p-value
hsa-miR-148a-3p	UCAGUGCACUACAGAACUUUGU	7.63E-04
hsa-miR-148b-3p	UCAGUGCAUCACAGAACUUUGU	7.63E-04
hsa-miR-19a-3p	UGUGCAAAUCUAUGCAAAACUGA	1.64E-03
hsa-miR-17-5p	CAAAGUGCUUACAGUGCAGGUAG	2.52E-03
hsa-miR-20b-5p	CAAAGUGCUCAUAGUGCAGGUAG	2.52E-03
hsa-miR-16-2-3p	CCAAUAUUACUGUGCUGCUUUA	3.54E-03
hsa-miR-147b-3p	GUGUGCGGAAAUGCUUCUGCUA	9.48E-03
hsa-miR-30a-5p	UGUAAACAUCCUCGACUGGAAG	2.04E-02
hsa-miR-30e-5p	UGUAAACAUCCUUGACUGGAAG	2.04E-02
hsa-miR-32-5p	AUUGCACAUUACUAAGUUGCA	2.25E-02
hsa-miR-98-5p	UGAGGUAGUAAGUUGUAUUGUU	3.42E-02
hsa-miR-429	UGCCAAAAUGGUCUGUCAUAAU	3.73E-02

Motif 2

miRNA	Sequence	p-value
hsa-miR-148a-3p	UCAGUGCACUACAGAACUUUGU	2.05E-05
hsa-miR-22-3p	AAGCUGCCAGUUGAAGAACUGU	2.24E-04
hsa-miR-10b-5p	UACCCUGUAGAACCGAAUUUGUG	2.38E-04
hsa-miR-19a-3p	UGCAAAUCUAUGCAAAACUGA	4.24E-04
hsa-miR-148b-3p	UCAGUGCAUCACAGAACUUUGU	1.67E-03
hsa-miR-151a-3p	CUAGACUGAAGCUCCUUGAGG	5.46E-03
hsa-miR-30a-5p	UGUAAACAUCCUCGACUGGAAG	1.40E-02
hsa-miR-30e-5p	UGUAAACAUCCUUGACUGGAAG	1.40E-02

Figure 5. *Motifs identified within the selectively exported microRNAs.* Motif discovery using the MEME algorithm revealed two enriched motifs detected from the selectively exported miRNA group. Tables shows the miRNAs containing the motif, position of motif (red) and p-value calculated from the sitemap algorithm. Motif 1 (top) matches to 12 of the 19 miRNAs in this group and motif 2 (bottom) matches 8 of the miRNAs.
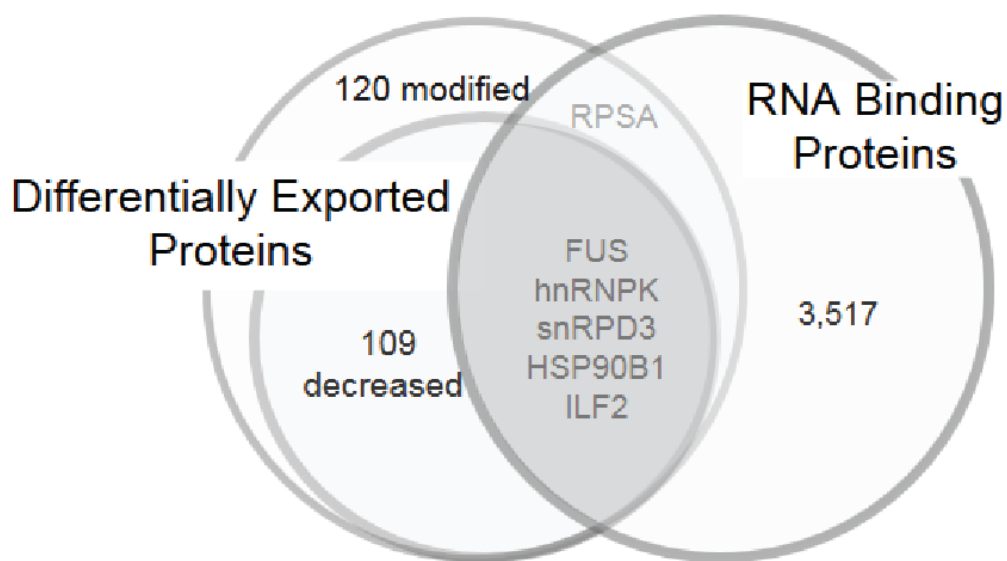
Figure 6: *Cavin-1 attenuates the EV export of RNA binding proteins*. MS/MS data compared the protein content of EVs between PC3 and PC3-cavin-1 cells to determine significantly (p≤0.05) differentially exported proteins. This is divided into proteins modified and proteins reduced in the EVs upon cavin-1 expression. Gene Ontology analysis revealed whether these exported proteins bind RNAs. Number of total RNA binding proteins reflects all human proteins with GO term, GO:0003723. 5 RNA binding proteins had reduced exported upon cavin-1 expression, shown by the shaded region.

of the hnRNP protein family had previously been implemented in miRNA export, focus was shifted to hnRNPK and FUS (also known as hnRNPP2). Interestingly, a recent study reported that hnRNPK specifically binds to the sequence AGUGUG in miR-122, through mutagenesis assays (Fan *et al.* 2015). The FIMO algorithm was used to compare the known motifs (Fig.5) to the sequence of miR-122. This analysis returned a significant match (p=0.0435) between the hnRNPK-binding region (AGUGUG) and the selective export motif 1. These computational results established hnRNPK as a viable candidate protein to mediate the selective export of miRNAs.
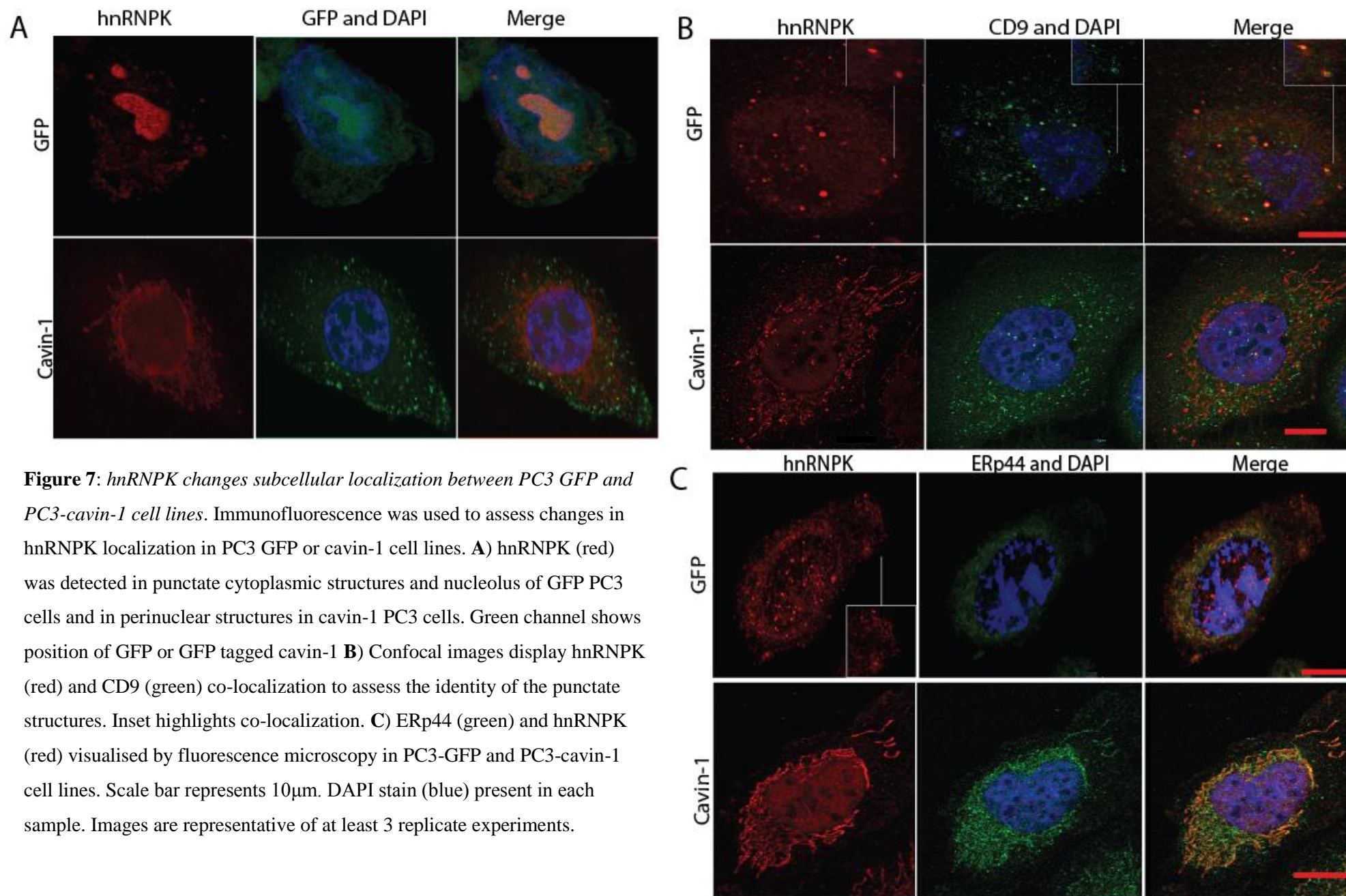
hnRNPK sub-cellular localization modified in cavin-1 PC3 line.

Heterogeneous Nuclear Ribonucleoprotein K (hnRNPK) is primarily a nuclear protein which is known to shuttle to the cytoplasm. Interestingly, several studies reportedhnRNPK in exosomes (REF). However, the subcellular localization of hnRNPK in PC3 cells, and the effect of cavin-1 on subcellular localization, is unknown. Determining hnRNPK subcellular localization may assist in understanding the differential export of hnRNPK and therefore its effect on miRNA export. Immunofluorescence was performed using anti-hnRNPK antibodies to determine its subcellular localization. Two different antibodies were initially tested, with similar results (data not shown). Thereafter, the rabbit anti-hnNPK antibody was used for all experiments. Strikingly, hnRNPK revealed a distinct change in localization between cell lines, from punctate-like structures in PC3-GFP to a perinuclear focus in PC3-cavin-1 cells (Fig.7a). The staining patterns suggested distribution to multivesicular bodies and endoplasmic rectiulum, respectively. Therefore, co-localization studies were performed with marker proteins CD9 and ERp44. hnRNPK appears to co-localize somewhat with the CD9 protein in GFP PC3 cells, which suggests potential presence in the multivesicular bodies (Fig.7b). However, the hnRNPK in PC3-cavin-1 cells was found present in endoplasmic reticulum, shown by strong overlap with ER resident protein, ERp44 (Fig.7c). No co-
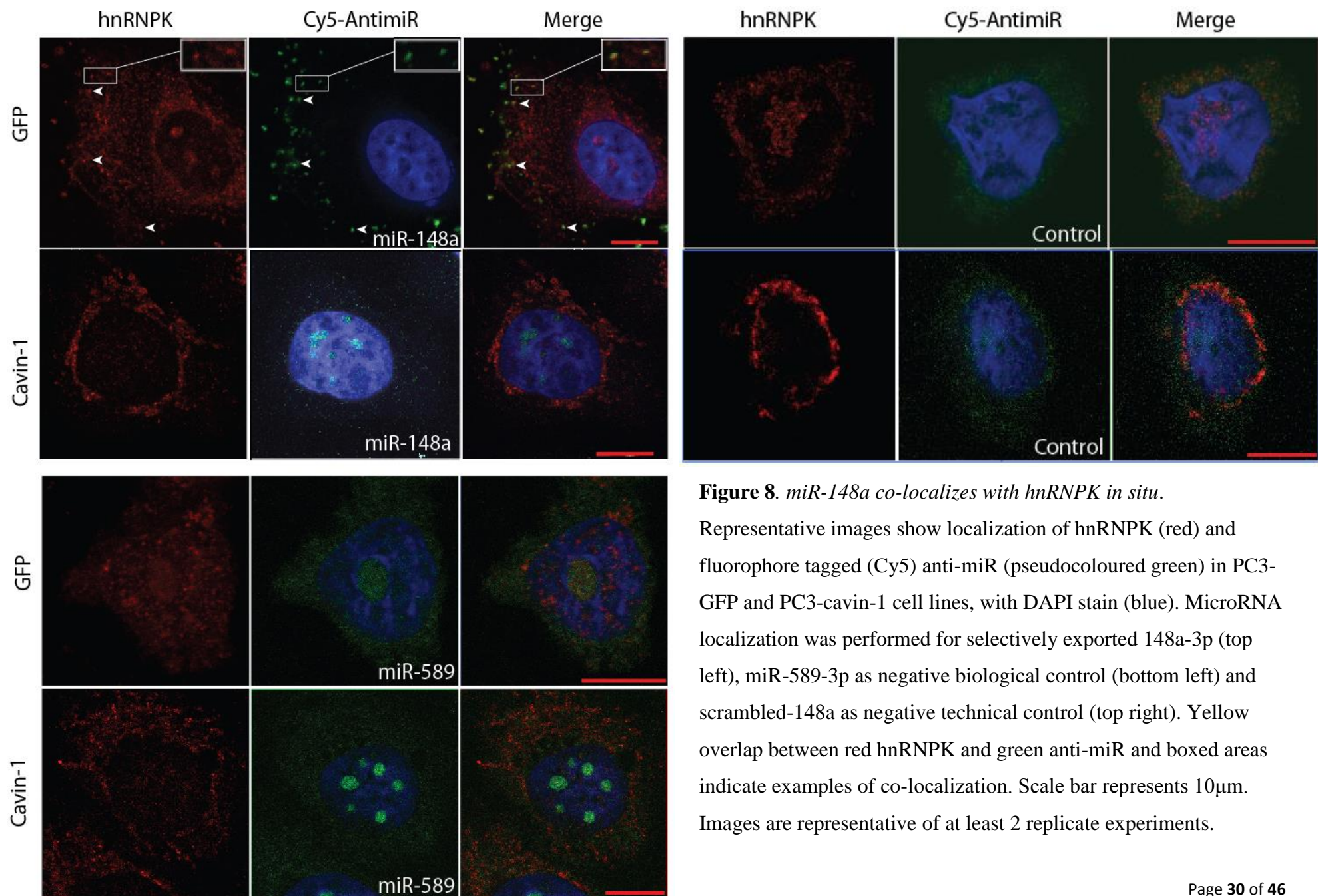
localization of hnRNPK with CD9 was observed in PC3-cavin-1 cells. Therefore, change in hnRNPK subcellular localization modified by cavin-1 expression could explain the differential export of hnRNPK and miRNAs.

hnRNPK co-localizes with selectively exported microRNAs.

hnRNPK has been reported to bind and interact with RNA, but so far there has been only one report of hnRNPK binding miRNA (Fan et al. 2015). The interaction between the selectively exported miRNAs and hnRNPK was assessed in two separate ways: by assessing co-localization by microRNA *in situ* hybridization with immunofluorescence (miR-ISH IF) and binding ability by RNA immunoprecipitation (RIP). miR-ISH IF methodology was established by modifying the existing Fluorescence *In Situ* Hybridization (FISH) methods and performing it with IF. The anti-miR probe highlights the target miRNAs based on RNA-RNA hybridization. Here, I assessed the subcellular co-localization of miR-148a-3p, 589-5p, a scrambled form of miR-148a (control) and hnRNPK (Fig.8). miR-148a was assessed as it contains the motif that hnRNPK was predicted to bind and possesses decreased export upon cavin-1 expression. In contrast, miR-589 was seen to be unaffected by expression of cavin-1 in EVs in RNA-seq analysis. This establishes a negative biological control that determines natural miRNA localization when not affected by selective export mechanism. Copies of pri-miR (primary microRNA transcript) for miR-148 and 589 are believed to be present in the nucleolus (Ritland Politz *et al.* 2009). Therefore the nucleolar localization of the Cy5 probes (excluding scrambled) confirms that the ISH was successful and that these miRNAs are expressed in these cells. As shown in Figure 8, miR-148a does seem to localize to punctate structures in the cytoplasm of PC3-GFP cell lines, presumably indicating presence in the multivesicular bodies that is not occurring in the PC3-cavin-1 cell lines. Interestingly, miR-148a co-localized with hnRNPK in PC3-GFP cells, shown by overlap towards the cells periphery (Fig.8). However no evidence of hnRNPK-miR-148 co-localization was observed

Figure 7: *hnRNPK changes subcellular localization between PC3 GFP and PC3-cavin-1 cell lines*. Immunofluorescence was used to assess changes in hnRNPK localization in PC3 GFP or cavin-1 cell lines. **A**) hnRNPK (red) was detected in punctate cytoplasmic structures and nucleolus of GFP PC3 cells and in perinuclear structures in cavin-1 PC3 cells. Green channel shows position of GFP or GFP tagged cavin-1 **B**) Confocal images display hnRNPK (red) and CD9 (green) co-localization to assess the identity of the punctate structures. Inset highlights co-localization. **C**) ERp44 (green) and hnRNPK (red) visualised by fluorescence microscopy in PC3-GFP and PC3-cavin-1 cell lines. Scale bar represents 10µm. DAPI stain (blue) present in each sample. Images are representative of at least 3 replicate experiments.

Figure 8. *miR-148a co-localizes with hnRNPK in situ*. Representative images show localization of hnRNPK (red) and fluorophore tagged (Cy5) anti-miR (pseudocoloured green) in PC3-GFP and PC3-cavin-1 cell lines, with DAPI stain (blue). MicroRNA localization was performed for selectively exported 148a-3p (top left), miR-589-3p as negative biological control (bottom left) and scrambled-148a as negative technical control (top right). Yellow overlap between red hnRNPK and green anti-miR and boxed areas indicate examples of co-localization. Scale bar represents 10μm. Images are representative of at least 2 replicate experiments.

in the PC3-cavin-1 cells (Fig. 8). Conversely, miR-589 displayed a non-specific localization in both cell lines, despite varying cell lines and hnRNPK localization. Lastly, control condition showed that the Cy5-scrambled-miR did not localize to the nucleolus or to any structures in particular (Fig. 8). Therefore, the concentrated fluorescent signal in punctate structures containing hnRNPK confirms co-localization of miR-148a and hnRNPK in GFP cells that is lacking in the PC3-cavin-1 cell line.

hnRNPK binds RNAs in the PC3 cell line.

Having demonstrated co-localization between hnRNPK with miR148a in PC3 cells, and the loss of this co-localization upon cavin-1 expression, next I attempted to demonstrate their direct interaction using immunoprecipitation (IP). Initial experiments were performed to confirm the specificity of the hnRNPK antibody by immunoblotting (not shown) and to optimize hnRNPK antibody coupling to protein G DynaBead, as well as using these beads for IP (not shown). As the RNA-protein interaction can be fairly transient, cellular material was crosslinked by formaldehyde prior to the co-IP. After elution from the IP beads, a western blot was performed to determine if IP conditions were suitable to pull down the targets of hnRNPK antibody (Fig.9a). This is observed as a band approximating 58-62kDa that reflects the native weight of hnRNPK. Additional bands at 70, 100, 125 and approximately 140kDa presumably reflect hnRNPK bound to various partners in this IP, including proteins, RNAs and miRNAs. Next, I attempted to purify the RNAs that hnRNPK binds. After purification by TRIzol extraction (which also reverses formaldehyde crosslinks), the RNA was quantified using Nanodrop. This yielded a consistent increase of RNA identified from the hnRNPK pull down compared to the IgG control (Fig.9b). This is consistent with past research that shows hnRNPK binding to RNAs and reports of it binding miRNAs (Klimek-Tomczak *et al.* 2004; Fan et al. 2015). While this is instrumental in determining whether hnRNPK binds to miRNAs, the low yield precludes RT-PCR of specific miRNAs. Due to time restrictions, a
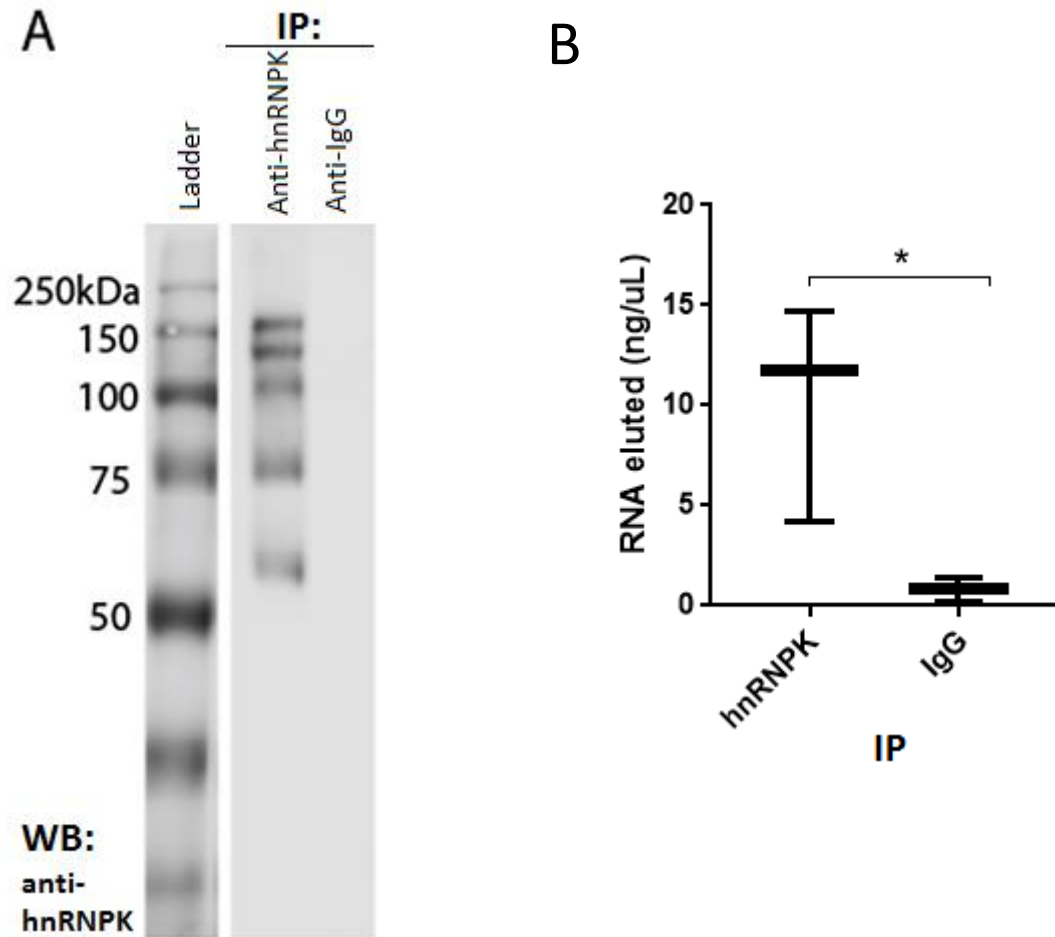
Figure 9: *hnRNPK binds RNA in PC3 cells.* **A)** Western blotting of anti-hnRNPK and anti-IgG immunoprecipitation experiment. Crosslinked protein from PC3 whole cell lysates was applied to rabbit hnRNPK or normal rabbit IgG antibody conjugated Dynabeads, eluted in SDS-page buffer, and blotted with mouse hnRNPK antibody to detect hnRNPK and its binding partners. Lane 2 (anti-hnRNPK) bands reflect the native weight of hnRNPK (≈60kDa) and hnRNPK bound material (≥75kDa) whereas lane 3 (control IgG) reveals no bands. **B)** Box and whisker plot displaying the nanodrop RNA quantification of RNA eluted from hnRNPK IP experiment. Each point summarises the mean, minimum and maximum RNA concentration (ng/μL) eluted from three IP experiments for anti-hnRNPK and IgG control. A two-sided Mann Whitney U-test revealed a significant (* p=0.0402) difference between test and control.

large scale experiment for RT-PCR was not able to be completed. Further assessment is needed to determine whether this population of RNA contains microRNAs and whether these miRs are the ones also predicted.

Discussion:

Circulating cancer-derived EVs are proposed as a source of protein and miRNA biomarkers, where EV cargo composition was previously thought to be representative of their cell of origin (Hunter *et al.* 2008; Choi *et al.* 2013). In contrast to this 'sampling' mechanism of EV cargo loading, our laboratory previously showed a 'selective export' mechanism for a subset of miRNA cargo (Inder et al. 2014). This project further evaluated the proposed selective export hypothesis using established prostate cancer cell models. Results from this study support this hypothesis where the RNA-binding protein hnRNPK binds to a subset of the EV miRNA content presumably via a conserved RNA-binding motif, AGUGCA, to traffic them to the multivesicular bodies to permit selective export via exosomes. Cavin-1 modulates this process by altering the subcellular location of hnRNPK to the endoplasmic reticulum (ER).

Interestingly, hnRNPK has been consistently associated with cancer progression. A review by Lu & Gao (2016) summarized its role in metastasis, where multiple reports link overexpression of hnRNPK with various mechanisms mediating metastasis such as invasion, reduction of apoptosis, angiogenesis and cell motility (Revil *et al.* 2009; Gao *et al.* 2013; Brown and Murray 2015). Some of these phenotypes are believed to be induced by transcriptional control mediated by mRNA-hnRNPK interactions, however further work is required to elucidate the roles of hnRNPK in metastasis (Habelhah *et al.* 2001; Notari *et al.* 2006). Additionally, hnRNPK is commonly found in EVs secreted from various cancer types, including late stage bladder, advanced prostate, metastatic colorectal and advanced brain cancers (Welton *et al.* 2010; Ji *et al.* 2013; Ramteke et al. 2015; Zhang *et al.* 2015). Yet, the

significance and function of EV hnRNPK in these cancers is unknown. Hereby, identifying

hnRNPK as a major mediator of EV miRNA content perhaps establishes a novel role and

function of EV hnRNPK in advanced cancers and elucidates some of the unknowns related to

miRNA regulation via subcellular compartmentalisation.

While hnRNPK is reported to be predominately nuclear based with cytoplasmic shuttling

ability, several studies had observed that hnRNPK in tumour cells possess aberrant

cytoplasmic localization (Proepper *et al.* 2011; Barboro *et al.* 2014). For example, hnRNPK

in advanced colorectal cancer possesses increased cytoplasmic accumulation and limited

nuclear localization (Hope and Murray 2011). This is consistent with the observed

localization in advanced prostate cancer PC3 cells (Fig. 7b). This study further resolved the

cytoplasmic hnRNPK localization to multivesicular bodies, which form exosomes. As the

proteomic data detected hnRNPK in EVs and past research consistently demonstrates

hnRNPK presence in cancer-derived exosomes, its presence in the MVBs was inferred

however never demonstrated until now. Interestingly, hnRNPK localizes predominantly in

the ER in PC3-cavin-1 cells. While this indicates that cavin-1 expression inflicts a change in

subcellular localization, hnRNPK has not been detected in the ER previously. Cavin-1 in PC3

cells may be inducing hnRNPK localization dissimilar to its usual phenotype. As the ER is

primarily the site of protein maturation and folding, perhaps cavin-1 is preventing hnRNPK

transport to its usual localization following translation thus retaining hnRNPK in the ER

(Kincaid and Cooper 2007). Retention to the ER would explain the reduction of EV hnRNPK

upon cavin-1 expression, though how cavin-1 induces hnRNPK ER retention is currently

unknown. Observations of hnRNPK in non-cancer prostate epithelial cells, such as the

RWPE-1 cell line which expresses caveolin-1 and cavin-1, would determine whether this ER

retention is a common function of cavin-1 or an abnormality found in only PC3-cavin-1 cell

lines. Nonetheless, the presented data suggest that subcellular localization of hnRNPK mediated by cavin-1 as a novel mechanism of regulating miRNA EV content.

Consistent with the hypothesis that hnRNPK binds and selectively exports miRNA, we detected miR-148a and hnRNPK co-localization at punctate cytoplasmic structures in PC3 cells, presumably MVBs. However, while hnRNPK changed localization in the cavin-1 positive cells, miR-148a didn't co-localize with it. This may suggest that cavin-1 is inflicting changes that prevents hnRNPK from interacting with miR-148a and its other targets, by inhibiting binding ability or spatial distribution. Furthermore, hnRNPK was not observed mediating the export of sampled miRNA, miR-589 in either cell line. miR-589 was analysed as its export did not change upon cavin-1 expression and does not contain the export motif and therefore should not bind to hnRNPK or be found in punctate structures. This reflects the null hypothesis of sampling, as the diffuse cytoplasmic miR-589 would simply be enveloped by forming EVs due to proximity. Therefore this study elucidated some of the underlying activity of the selective export miRNA mechanism and demonstrated the miRNA cellular distribution required for sampling.

While the link between cavin-1 expression and hnRNPK activity is still unknown, several hypotheses were formed to explain the change in hnRNPK activity and potential links. From this study, we identified that cavin-1 regulates miRNA export through the presence or absence of hnRNPK in the MVB. Commonly, localization changes occur though modifications of localization signals, often achieved through post-translational modification (Eisenhaber and Eisenhaber 2007). When investigated, hnRNPK and many of the members of the hnRNP family undergo SUMOylation where this modification alters hnRNPK nuclear translocation (Lee *et al.* 2012). The site of SUMOylation, Lys422, overlaps with the third K-homology domain, one of four RNA-binding sites of hnRNPK (3 KH domains and 1 RGG-box) (Paziewska *et al.* 2004; Lee et al. 2012). This may potentially serve as the reason that

both subcellular localization and reduced interaction is occurring between hnRNPK and miR-148a in the cavin-1 PC3 cells. Furthermore, Villarroya-Beltri *et al* (2013) found that the interaction between their hnRNP protein and miRNA binding affinity was dependant on SUMOlyation. Though, to our knowledge no direct link is found between cavin-1 and SUMOlyation. For these reasons, identifying hnRNPK post translational modifications may be beneficial in understanding the regulation of hnRNPK to the EVs and the miRNA export.

A potential link between cavin-1 expression and hnRNPK function may lie in lipid raft composition. Lipid rafts are microdomains that are enriched in specific lipids, such as cholesterol, ceramide and sphingolipid, where this composition dictates protein composition (Harder *et al.* 1998). Raft lipids are found in EVs, the membrane of the ER, Golgi bodies and in the plasma membrane (Alonso and Millán 2001). Earlier studies revealed that expression of cavin-1 in PC3 cell lines reduces the amount of cholesterol found in lipid rafts, resulting in a change in lipid and protein composition (Inder et al. 2012). This included modulation of hnRNPK recruitment to these microdomains (Inder et al. 2012). Hence it is possible that cavin-1 expression reduced the recruitment of hnRNPK to extracellular vesicle lipid rafts, MVB and exosomes in PC3 cells. Future studies are required to identify the link between cavin-1 and hnRNPK.

It should also be noted that while this study analysed the mixed population of EVs, the localization of hnRNPK seems to indicate a preference for MVBs which precede the formation of exosomes. The lack of recruitment of hnRNPK to the plasma membrane suggests that hnRNPK export may be predominately through exosome release rather than microvesicles. This distinction is important in vesicle research to define differences between EV subpopulations where some studies state subpopulations may have varying roles (Evans-Osses *et al.* 2015). A 2014 study determined the miRNA and protein content of EVs from colon cancer was different in different EV subpopulations (Tauro *et al.* 2013; Ji *et al.* 2014),

indicating that some methods of export are specific to each vesicle type. However, the functional difference of these subpopulations has not been identified. Still, this finding contributes to the understanding of exosome specific export mechanisms.

While this study analysed the role of hnRNPK in miRNA EV export, it is likely that several RNA binding proteins interact collaboratively to achieve the export of the miRNAs. The analysis of previously published proteomic data from our lab revealed 5 candidate RNA-binding proteins that may be involved in this export mechanism; hnRNPK was chosen as the candidate for further investigation as its reported target RNA sequence matched to the selective export motif. FUS, another member of the hnRNP family, was not further analysed in this study merely for the fact that current RNA binding information is inadequate to determine accurate binding predictions (Lerga *et al.* 2001). However, considering that members of the hnRNP family usually interact in complexes, it is plausible to suggest that these proteins are working together to mediate the export (Krecic and Swanson 1999). Wang *et al* (2014) confirmed that hnRNPK and FUS interact directly. Furthermore, the selective export motif identified that relates to hnRNPK, AGUGCA, did not correspond to all of the selectively exported miRNAs (Fig 5). Together, this suggests that multiple proteins could be working collaboratively to populate the EVs. Therefore, analysing the interaction between hnRNPK, FUS, miRNAs and other potential RNA-binding proteins in future research may assist in further understanding the mechanism.

Although the function of the selectively exported miRNAs were not assessed in this report, surveying the literature reveals that many of these miRNAs possess roles associated with cancer and cancer progression. Huang *et al.* (2014) determined that miR-98, 148b, 30e, 30a, 148a, 3615 and 20b contribute to immune response regulation in papillary thyroid carcinoma. Additionally, miR-22, 200a and 429 were found to be involved with epithelial to mesenchyme transition in various cancers (Pola 2013; Pichler *et al.* 2014; Yan *et al.* 2015).

This suggests that these miRNAs play roles in modifying the tumour microenvironment and establishment of the pre-metastatic niche. This is consistent with past research that linked EV contained miRNAs with these pro-metastatic functions (Milane *et al.* 2015). Therefore this miRNA export mechanism may be key in modulating the pro-metastatic phenotype associated with EV secretion in this advanced prostate cancer cell line.

The hnRNPK and miRNA interaction is predicted to be mediated by the selective export motif (motif 1, Fig. 5). Interesting, this motif seemed to predominately match within the first 10 nucleotides of its target miRNA. Position 2-10 of a miRNA is known as the seed region and is believed to be the canonical binding site that mediates the specific miRNA-mRNA interactions (Mullany *et al.* 2016). Therefore, these miRNAs will not be able to perform their canonical function whilst bound to hnRNPK. The regulatory processes that mediate miRNA function after processing are not fully known (Zhang *et al.* 2012), therefore identifying proteins that can inhibit the canonical binding site or modulate compartmentalisation of miRNAs can contribute to our understanding of miRNA regulation. However, as the motif location is not consistent across all miRNAs predicted to bind to hnRNPK, it is unlikely to be a robust function. Nonetheless, this may provide as an additional miRNA regulatory function induced hnRNPK in combination with modulating export.

Several technical limitations were encountered during this study, which should be further investigated in future work. Attempts to validate the EV and cellular miRNA levels was completed using RT-qPCR. While the trends from the RNA-seq data was maintained for these validated miRNAs, high variation of the EV data was observed. Unfortunately, this appears to be an issue with the low quantities of miRNAs extracted from the EVs in combination with the RT-qPCR sensitivity limitation. Ideally, repeating this experiment using more sensitive count based methods such as the digital droplet PCR (ddPCR), as described by Chevillet *et al.* (2014), would limit this variation. Furthermore, experimental demonstration

of the direct binding between hnRNPK and selectively exported miRNAs such as miR-148a could not be completed due to time constraints and the low yield of pulldowns. Confirming binding interaction assists in determining whether these do indeed directly interact as the co-localization experiments infer. Additionally, combining the pulldown with ddPCR and potentially sequencing can reveal whether the motif predictions were indeed correct. Given that motif discovery is a method to identify binding sites based on probabilistic models, some predictions may be false positives (Hu *et al.* 2005), and therefore experimental validation will be required. Ultimately, this will provide a clearer understanding of the selectivity of hnRNPK to mediate the selective export of miRNAs.

In conclusion, this study has identified a viable export protein that can mediate the selective export of miRNAs to EVs, specifically exosomes, in prostate cancer cell lines. hnRNPK was found to modulate the selective export of miR-148a, and is predicted to mediate additional miRNAs, where expression of cavin-1 prevents its appropriate MVB localization to fulfil this function. However, the underlying link between cavin-1 and hnRNPK function/localization is currently unknown. Future efforts to identify this link and validate some of the interactions is required. Ultimately, identifying this mechanism assists in understanding how pro-oncogenic miRNAs are regulated in the EVs to facilitate their role in cancer progression but also, details some of the underlying mechanisms mediating miRNAs and exosome cargo sorting.

References:

Alonso, M. A. and J. Millán (2001). "The role of lipid rafts in signalling and membrane trafficking in T lymphocytes." Journal of Cell Science **114**(22): 3957.

Aung, C. S., M. M. Hill, M. Bastiani, R. G. Parton and M. O. Parat (2011). "PTRF-cavin-1 expression decreases the migration of PC3 prostate cancer cells: role of matrix metalloprotease 9." Eur J Cell Biol **90**(2-3): 136-42.

Balcells, I., S. Cirera and P. K. Busk (2011). "Specific and sensitive quantitative RT-PCR of miRNAs with DNA primers." BMC Biotechnology **11**(1): 1-11.

Barboro, P., N. Ferrari and C. Balbi (2014). "Emerging roles of heterogeneous nuclear ribonucleoprotein K (hnRNP K) in cancer progression." Cancer Letters **352**(2): 152-9.

Brown, G. T. and G. I. Murray (2015). "Current mechanistic insights into the roles of matrix metalloproteinases in tumour invasion and metastasis." J Pathol **237**(3): 273-81.

Bubendorf, L., A. Schöpfer, U. Wagner, G. Sauter, H. Moch, N. Willi, T. C. Gasser and M. J. Mihatsch (2000). "Metastatic patterns of prostate cancer: An autopsy study of 1,589 patients." Human Pathology **31**(5): 578-83.

Chatterjee, M., E. Ben-Josef, D. G. Thomas, M. A. Morgan, M. M. Zalupski, G. Khan, C. Andrew Robinson, K. A. Griffith, C.-S. Chen, T. Ludwig, T. Bekaii-Saab, A. Chakravarti and T. M. Williams (2015). "Caveolin-1 is Associated with Tumor Progression and Confers a Multi-Modality Resistance Phenotype in Pancreatic Cancer." Scientific Reports **5**: 10867.

Cheng, P., C. Chen, H. B. He, R. Hu, H. D. Zhou, H. Xie, W. Zhu, R. C. Dai, X. P. Wu, E. Y. Liao and X. H. Luo (2013). "miR-148a regulates osteoclastogenesis by targeting V-maf musculoaponeurotic fibrosarcoma oncogene homolog B." J Bone Miner Res **28**(5): 1180-90.

Chevillet, J. R., Q. Kang, I. K. Ruf, H. A. Briggs, L. N. Vojtech, S. M. Hughes, H. H. Cheng, J. D. Arroyo, E. K. Meredith, E. N. Gallichotte, E. L. Pogosova-Agadjanyan, C. Morrissey, D. L. Stirewalt, F. Hladik, E. Y. Yu, C. S. Higano and M. Tewari (2014). "Quantitative and stoichiometric analysis of the microRNA content of exosomes." Proceedings of the National Academy of Sciences **111**(41): 14888-93.

Choi, D. S., J. Lee, G. Go, Y. K. Kim and Y. S. Gho (2013). "Circulating extracellular vesicles in cancer diagnosis and monitoring: an appraisal of clinical potential." Mol Diagn Ther **17**(5): 265-71.

Costa-Silva, B., N. M. Aiello, A. J. Ocean, S. Singh, H. Zhang, B. K. Thakur, A. Becker, A. Hoshino, M. T. Mark, H. Molina, J. Xiang, T. Zhang, T.-M. Theilen, G. Garcia-Santos, C. Williams, Y. Ararso, Y. Huang, G. Rodrigues, T.-L. Shen, K. J. Labori, I. M. B. Lothe, E. H. Kure, J. Hernandez, A. Doussot, S. H. Ebbesen, P. M. Grandgenett, M. A. Hollingsworth, M. Jain, K. Mallya, S. K. Batra, W. R. Jarnagin, R. E. Schwartz, I. Matei, H. Peinado, B. Z. Stanger, J. Bromberg and D. Lyden (2015). "Pancreatic cancer exosomes initiate pre-metastatic niche formation in the liver." Nat Cell Biol **17**(6): 816-26.

Djuranovic, S., A. Nahvi and R. Green (2012). "miRNA-Mediated Gene Silencing by Translational Repression Followed by mRNA Deadenylation and Decay." Science **336**(6078): 237-40.

Dovrat, S., M. Caspi, A. Zilberberg, L. Lahav, A. Firsow, H. Gur and R. Rosin-Arbesfeld (2014). "14-3-3 and β-catenin are secreted on extracellular vesicles to activate the oncogenic Wnt pathway." Molecular Oncology **8**(5): 894-911.

Dreyfuss, G., V. N. Kim and N. Kataoka (2002). "Messenger-RNA-binding proteins and the messages they carry." Nat Rev Mol Cell Biol **3**(3): 195-205.

Eisenhaber, B. and F. Eisenhaber (2007). "Posttranslational modifications and subcellular localization signals: indicators of sequence regions without inherent 3D structure?" Curr Protein Pept Sci **8**(2): 197-203.

Evans-Osses, I., L. H. Reichembach and M. I. Ramirez (2015). "Exosomes or microvesicles? Two kinds of extracellular vesicles with different routes to modify protozoan-host cell interaction." Parasitol Res **114**(10): 3567-75.

Fan, B., F. X. Sutandy, G. D. Syu, S. Middleton, G. Yi, K. Y. Lu, C. S. Chen and C. C. Kao (2015). "Heterogeneous Ribonucleoprotein K (hnRNP K) Binds miR-122, a Mature Liver-Specific MicroRNA Required for Hepatitis C Virus Replication." Mol Cell Proteomics **14**(11): 2878-86.

Friedman, R. C., K. K. Farh, C. B. Burge and D. P. Bartel (2009). "Most mammalian mRNAs are conserved targets of microRNAs." Genome Res **19**(1): 92-105.

Gao, R., Y. Yu, A. Inoue, N. Widodo, S. C. Kaul and R. Wadhwa (2013). "Heterogeneous nuclear ribonucleoprotein K (hnRNP-K) promotes tumor metastasis by induction of genes involved in extracellular matrix, cell movement, and angiogenesis." J Biol Chem **288**(21): 15046-56.

Grande-García, A., A. Echarri, J. de Rooij, N. B. Alderson, C. M. Waterman-Storer, J. M. Valdivielso and M. A. del Pozo (2007). "Caveolin-1 regulates cell polarization and directional migration through Src kinase and Rho GTPases." The Journal of Cell Biology **177**(4): 683-94.

Gumulec, J., J. Sochor, M. Hlavna, M. Sztalmachova, S. Krizkova, P. Babula, R. Hrabec, A. Rovny, V. Adam, T. Eckschlager, R. Kizek and M. Masarik (2012). "Caveolin-1 as a potential high-risk prostate cancer biomarker." Oncology Reports **27**(3): 831-41.

Ha, M. and V. N. Kim (2014). "Regulation of microRNA biogenesis." Nat Rev Mol Cell Biol **15**(8): 509-24.

Habelhah, H., K. Shah, L. Huang, A. Ostareck-Lederer, A. L. Burlingame, K. M. Shokat, M. W. Hentze and Z. e. Ronai (2001). "ERK phosphorylation drives cytoplasmic accumulation of hnRNP-K and inhibition of mRNA translation." Nat Cell Biol **3**(3): 325-30.

Hansen, C. G., N. A. Bright, G. Howard and B. J. Nichols (2009). "SDPR induces membrane curvature and functions in the formation of caveolae." Nature Cell Biology **11**(7): 807-14.

Harder, T., P. Scheiffele, P. Verkade and K. Simons (1998). "Lipid Domain Structure of the Plasma Membrane Revealed by Patching of Membrane Components." The Journal of Cell Biology **141**(4): 929-42.

Hayashi, T., T. Ichimura, N. Yaegashi, T. Shiozawa and I. Konishi (2015). "Expression of CAVEOLIN 1 in uterine mesenchymal tumors: No relationship between malignancy and CAVEOLIN 1 expression." Biochemical and Biophysical Research Communications **463**(4): 982-7.

Hedlund, M., O. Nagaeva, D. Kargl, V. Baranov and L. Mincheva-Nilsson (2011). "Thermal- and Oxidative Stress Causes Enhanced Release of NKG2D Ligand-Bearing Immunosuppressive Exosomes in Leukemia/Lymphoma T and B Cells." PLoS ONE **6**(2): e16899.

Hill, M. M., M. Bastiani, R. Luetterforst, M. Kirkham, A. Kirkham, S. J. Nixon, P. Walser, D. Abankwa, V. M. J. Oorschot, S. Martin, J. F. Hancock and R. G. Parton (2008). "PTRF-Cavin, a Conserved Cytoplasmic Protein Required for Caveola Formation and Function." Cell **132**(1): 113-24.

Hope, N. R. and G. I. Murray (2011). "The expression profile of RNA-binding proteins in primary and metastatic colorectal cancer: relationship of heterogeneous nuclear ribonucleoproteins with prognosis." Human Pathology **42**(3): 393-402.

Hu, J., B. Li and D. Kihara (2005). "Limitations and potentials of current motif discovery algorithms." Nucleic Acids Research **33**(15): 4899-913.

Huang, C.-T., Y.-J. Oyang, H.-C. Huang and H.-F. Juan (2014). "MicroRNA-mediated networks underlie immune response regulation in papillary thyroid carcinoma." Scientific Reports **4**: 6495.

Hunter, M. P., N. Ismail, X. Zhang, B. D. Aguda, E. J. Lee, L. Yu, T. Xiao, J. Schafer, M.-L. T. Lee, T. D. Schmittgen, S. P. Nana-Sinkam, D. Jarjoura and C. B. Marsh (2008). "Detection of microRNA Expression in Human Peripheral Blood Microvesicles." PLoS ONE **3**(11): e3694.

Inder, K. L., J. E. Ruelcke, L. Petelin, H. Moon, E. Choi, J. Rae, A. Blumenthal, D. Hutmacher, N. A. Saunders, J. L. Stow, R. G. Parton and M. M. Hill (2014). "Cavin-1/PTRF alters prostate cancer cell-derived extracellular vesicle content and internalization to attenuate extracellular vesicle-mediated osteoclastogenesis and osteoblast proliferation." J Extracell Vesicles **3**.

Inder, K. L., Y. Z. Zheng, M. J. Davis, H. Moon, D. Loo, H. Nguyen, J. A. Clements, R. G. Parton, L. J. Foster and M. M. Hill (2012). "Expression of PTRF in PC-3 Cells modulates cholesterol dynamics and the actin cytoskeleton impacting secretion pathways." Mol Cell Proteomics **11**(2): M111.012245.

Ji, H., M. Chen, D. W. Greening, W. He, A. Rai, W. Zhang and R. J. Simpson (2014). "Deep Sequencing of RNA from Three Different Extracellular Vesicle (EV) Subtypes Released from the Human LIM1863 Colon Cancer Cell Line Uncovers Distinct Mirna-Enrichment Signatures." PLoS ONE **9**(10): e110314.

Ji, H., D. W. Greening, T. W. Barnes, J. W. Lim, B. J. Tauro, A. Rai, R. Xu, C. Adda, S. Mathivanan, W. Zhao, Y. Xue, T. Xu, H.-J. Zhu and R. J. Simpson (2013). "Proteome profiling of exosomes

derived from human primary and metastatic colorectal cancer cells reveal differential expression of key metastatic factors and signal transduction components." PROTEOMICS **13**(10-11): 1672-86.

Kharmate, G., E. Hosseini-Beheshti, J. Caradec, M. Y. Chin and E. S. Tomlinson Guns (2016). "Epidermal Growth Factor Receptor in Prostate Cancer Derived Exosomes." PLoS ONE **11**(5): e0154967.

Kincaid, M. M. and A. A. Cooper (2007). "Misfolded Proteins Traffic from the Endoplasmic Reticulum (ER) Due to ER Export Signals." Mol Biol Cell **18**(2): 455-63.

Klimek-Tomczak, K., L. S. Wyrwicz, S. Jain, K. Bomsztyk and J. Ostrowski (2004). "Characterization of hnRNP K protein-RNA interactions." J Mol Biol **342**(4): 1131-41.

Kosaka, N., H. Iguchi, Y. Yoshioka, F. Takeshita, Y. Matsuki and T. Ochiya (2010). "Secretory mechanisms and intercellular transfer of microRNAs in living cells." J Biol Chem **285**(23): 17442-52.

Krecic, A. M. and M. S. Swanson (1999). "hnRNP complexes: composition, structure, and function." Curr Opin Cell Biol **11**(3): 363-71.

Lee, J. T. Y., W. H. Tsang and K. L. Chow (2011). "Simple Modifications to Standard TRIzol® Protocol Allow High-Yield RNA Extraction from Cells on Resorbable Materials." Journal of Biomaterials and Nanobiotechnology **02**(01): 41-8.

Lee, S. W., M. H. Lee, J. H. Park, S. H. Kang, H. M. Yoo, S. H. Ka, Y. M. Oh, Y. J. Jeon and C. H. Chung (2012). "SUMOylation of hnRNP-K is required for p53-mediated cell-cycle arrest in response to DNA damage." The EMBO Journal **31**(23): 4441-52.

Lerga, A., M. Hallier, L. Delva, C. Orvain, I. Gallais, J. Marie and F. Moreau-Gachelin (2001). "Identification of an RNA Binding Specificity for the Potential Splicing Factor TLS." Journal of Biological Chemistry **276**(9): 6807-16.

Lu, J. and F. H. Gao (2016). "Role and molecular mechanism of heterogeneous nuclear ribonucleoprotein K in tumor development and progression." Biomed Rep **4**(6): 657-63.

Luz, M. A. and A. G. Aprikian (2010). "Preventing bone complications in advanced prostate cancer." Current Oncology **17**(Suppl 2): S65-S71.

McKechnie, N. M., B. C. R. King, E. Fletcher and G. Braun (2006). "Fas-ligand is stored in secretory lysosomes of ocular barrier epithelia and released with microvesicles." Experimental Eye Research **83**(2): 304-14.

McMahon, K.-A., H. Zajicek, W.-P. Li, M. J. Peyton, J. D. Minna, V. J. Hernandez, K. Luby-Phelps and R. G. W. Anderson (2009). "SRBC/cavin-3 is a caveolin adapter protein that regulates caveolae function." The EMBO Journal **28**(8): 1001-15.

Milane, L., A. Singh, G. Mattheolabakis, M. Suresh and M. M. Amiji (2015). "Exosome mediated communication within the tumor microenvironment." J Control Release **219**: 278-94.

Mili, S., H. J. Shu, Y. Zhao and S. Pinol-Roma (2001). "Distinct RNP complexes of shuttling hnRNP proteins with pre-mRNA and mRNA: candidate intermediates in formation and export of mRNA." Mol Cell Biol **21**(21): 7307-19.

Montecalvo, A., A. T. Larregina, W. J. Shufesky, D. B. Stolz, M. L. Sullivan, J. M. Karlsson, C. J. Baty, G. A. Gibson, G. Erdos, Z. Wang, J. Milosevic, O. A. Tkacheva, S. J. Divito, R. Jordan, J. Lyons-Weiler, S. C. Watkins and A. E. Morelli (2012). "Mechanism of transfer of functional microRNAs between mouse dendritic cells via exosomes." Blood **119**(3): 756-66.

Moon, H., C. S. Lee, K. L. Inder, S. Sharma, E. Choi, D. M. Black, K. A. Le Cao, C. Winterford, J. I. Coward, M. T. Ling, D. J. Craik, R. G. Parton, P. J. Russell and M. M. Hill (2014). "PTRF/cavin-1 neutralizes non-caveolar caveolin-1 microdomains in prostate cancer." Oncogene **33**(27): 3561-70.

Moumita, C., B.-J. Edgar, G. T. Dafydd, A. M. Meredith, M. Z. Mark, K. Gazala, R. Charles Andrew, A. G. Kent, C. Ching-Shih, L. Thomas, B.-S. Tanios, C. Arnab and M. W. Terence (2015). "Caveolin-1 is Associated with Tumor Progression and Confers a Multi-Modality Resistance Phenotype in Pancreatic Cancer." Scientific Reports **5**.

Mullany, L. E., J. S. Herrick, R. K. Wolff and M. L. Slattery (2016). "MicroRNA Seed Region Length Impact on Target Messenger RNA Expression and Survival in Colorectal Cancer." PLoS ONE **11**(4): e0154177.

Notari, M., P. Neviani, R. Santhanam, B. W. Blaser, J. S. Chang, A. Galietta, A. E. Willis, D. C. Roy, M. A. Caligiuri, G. Marcucci and D. Perrotti (2006). "A MAPK/HNRPK pathway controls BCR/ABL oncogenic potential by regulating MYC mRNA translation." Blood **107**(6): 2507-16.

Palma, J., S. C. Yaddanapudi, L. Pigati, M. A. Havens, S. Jeong, G. A. Weiner, K. M. E. Weimer, B. Stern, M. L. Hastings and D. M. Duelli (2012). "MicroRNAs are exported from malignant cells in customized particles." Nucleic Acids Research **40**(18): 9125-38.

Paziewska, A., L. S. Wyrwicz, J. M. Bujnicki, K. Bomsztyk and J. Ostrowski (2004). "Cooperative binding of the hnRNP K three KH domains to mRNA targets." FEBS letters **577**(1–2): 134-40.

Pegtel, D. M., L. Peferoen and S. Amor (2014). "Extracellular vesicles as modulators of cell-to-cell communication in the healthy and diseased brain." Philosophical Transactions of the Royal Society B: Biological Sciences **369**(1652): 20130516.

Pichler, M., A. L. Ress, E. Winter, V. Stiegelbauer, M. Karbiener, D. Schwarzenbacher, M. Scheideler, C. Ivan, S. W. Jahn, T. Kiesslich, A. Gerger, T. Bauernhofer, G. A. Calin and G. Hoefler (2014). "MiR-200a regulates epithelial to mesenchymal transition-related gene expression and determines prognosis in colorectal cancer patients." Br J Cancer **110**(6): 1614-21.

Pola, C. (2013). "Cancer: miR-22 attacks on several fronts." Nat Med **19**(8): 980-.

Proepper, C., K. Steinestel, M. J. Schmeisser, J. Heinrich, J. Steinestel, J. Bockmann, S. Liebau and T. M. Boeckers (2011). "Heterogeneous Nuclear Ribonucleoprotein K Interacts with Abi-1 at Postsynaptic Sites and Modulates Dendritic Spine Morphology." PLoS ONE **6**(11): e27045.

Ramteke, A., H. Ting, C. Agarwal, S. Mateen, R. Somasagara, A. Hussain, M. Graner, B. Frederick, R. Agarwal and G. Deep (2015). "Exosomes secreted under hypoxia enhance invasiveness and stemness of prostate cancer cells by targeting adherens junction molecules." Mol Carcinog **54**(7): 554-65.

Reddi, K. K. and J. F. Holland (1976). "Elevated serum ribonuclease in patients with pancreatic cancer." Proceedings of the National Academy of Sciences **73**(7): 2308-10.

Revil, T., J. Pelletier, J. Toutant, A. Cloutier and B. Chabot (2009). "Heterogeneous Nuclear Ribonucleoprotein K Represses the Production of Pro-apoptotic Bcl-x(S) Splice Isoform." J Biol Chem **284**(32): 21458-67.

Ritland Politz, J. C., E. M. Hogan and T. Pederson (2009). "MicroRNAs with a nucleolar location." RNA **15**(9): 1705-15.

Song, X., Y. Ding, G. Liu, X. Yang, R. Zhao, Y. Zhang, X. Zhao, G. J. Anderson and G. Nie (2016). "Cancer Cell-Derived Exosomes Induce Mitogen-Activated Protein Kinase-Dependent Monocyte Survival by Transport of Functional Receptor Tyrosine Kinases." Journal of Biological Chemistry.

Tauro, B. J., D. W. Greening, R. A. Mathias, S. Mathivanan, H. Ji and R. J. Simpson (2013). "Two Distinct Populations of Exosomes Are Released from LIM1863 Colon Carcinoma Cell-derived Organoids." Mol Cell Proteomics **12**(3): 587-98.

Towbin, H., T. Staehelin and J. Gordon (1979). "Electrophoretic transfer of proteins from polyacrylamide gels to nitrocellulose sheets: procedure and some applications." Proc Natl Acad Sci U S A **76**(9): 4350-4.

Tsui, N. B., E. K. Ng and Y. M. Lo (2002). "Stability of endogenous and added RNA in blood specimens, serum, and plasma." Clin Chem **48**(10): 1647-53.

Villarroya-Beltri, C., C. Gutiérrez-Vázquez, F. Sánchez-Cabo, D. Pérez-Hernández, J. Vázquez, N. Martin-Cofreces, D. J. Martinez-Herrera, A. Pascual-Montano, M. Mittelbrunn and F. Sánchez-Madrid (2013). "Sumoylated hnRNPA2B1 controls the sorting of miRNAs into exosomes through binding to specific motifs." Nat Commun **4**.

Wang, R., Z. Li, H. Guo, W. Shi, Y. Xin, W. Chang and T. Huang (2014). "Caveolin 1 knockdown inhibits the proliferation, migration and invasion of human breast cancer BT474 cells." Mol Med Rep **9**(5): 1723-8.

Welton, J. L., S. Khanna, P. J. Giles, P. Brennan, I. A. Brewis, J. Staffurth, M. D. Mason and A. Clayton (2010). "Proteomics analysis of bladder cancer exosomes." Mol Cell Proteomics **9**(6): 1324-38.

Wu, H.-C., C.-H. Chang, Y.-A. Tsou, C.-W. Tsai, C.-C. Lin and D.-T. Bau (2011). "Significant Association of Caveolin-1 (CAV1) Genotypes with Prostate Cancer Susceptibility in Taiwan." Anticancer Research **31**(2): 745-9.

Wysoczynski, M. and M. Z. Ratajczak (2009). "LUNG CANCER SECRETED MICROVESCILES: UNDERAPPRECIATED MODULATORS OF MICROENVIRONMENT IN EXPANDING TUMORS." International journal of cancer. Journal international du cancer **125**(7): 1595-603.

Yan, Y., Q. Wang, X.-L. Yan, Y. Zhang, W. Li, F. Tang, X. Li and P. Yang (2015). "miR-10a controls glioma migration and invasion through regulating epithelial–mesenchymal transition via EphA8." FEBS letters **589**(6): 756-65.

Zhang, P., Z. Guo, Y. Zhang, Z. Gao, N. Ji, D. Wang, L. Zou, W. Sun and L. Zhang (2015). "A preliminary quantitative proteomic analysis of glioblastoma pseudoprogression." Proteome science **13**(1): 12.

Zhang, Z., Y.-W. Qin, G. Brewer and Q. Jing (2012). "MicroRNA degradation and turnover: regulating the regulators." Wiley interdisciplinary reviews. RNA **3**(4): 593-600.

Zhou, W., M. Y. Fong, Y. Min, G. Somlo, L. Liu, M. R. Palomares, Y. Yu, A. Chow, S. T. F. O'Connor, A. R. Chin, Y. Yen, Y. Wang, E. G. Marcusson, P. Chu, J. Wu, X. Wu, A. X. Li, Z. Li, H. Gao, X. Ren, M. P. Boldin, P. C. Lin and S. E. Wang (2014). "Cancer-secreted miR-105 destroys vascular endothelial barriers to promote metastasis." Cancer Cell **25**(4): 501-15.